Inhibition of colorectal cancer tumorigenesis by ursolic acid and doxorubicin is mediated by targeting the Akt signaling pathway and activating the Hippo signaling pathway

DAN HU[1], RUO YU MENG[1], THI VAN NGUYEN[2], OK HEE CHAI[2], BYUNG HYUN PARK[3], JU-SEOG LEE[4] and SOO MI KIM[1]

Departments of [1]Physiology, [2]Anatomy and [3]Biochemistry, Jeonbuk National University Medical School, Jeonju, Jeollabuk-do 54907, Republic of Korea; [4]Department of Systems Biology, The University of Texas MD Anderson Cancer Center, Houston, TX 77030, USA

Received May 31, 2022; Accepted September 16, 2022

DOI: 10.3892/mmr.2022.12898

Abstract. Colorectal cancer (CRC) is one of the deadliest malignant tumors worldwide and its prevalence is increasing in South Korea. The efficacy of combined treatment with natural product-derived and chemotherapy agents including curcumin combined with 5-fluorouracil, resveratrol combined with cisplatin and epigallocatechin-3-gallate (EGCG) combined with cisplatin in preventing cancer progression and killing cancer cells has emerged. The Akt and Hippo signaling pathways serve a key role in colorectal tumor growth; however, the exact role of the crosstalk between Akt and Hippo signaling pathways in CRC remains poorly elucidated. The combined effect of UA and DOX on the cell proliferation, apoptosis, migration and cell cycle of CRC cells were investigated by performing Cell proliferation assay, a soft agar colony formation assay, flow cytometry, wound healing assay and western blotting assay. Subsequently, the expression of AKT and Hippo signaling pathway-associated proteins were also assessed by western blot assay. Moreover, a xenograft nude mouse model was constructed to verify the effects of UA and DOX on the tumorigenesis of HCT116 cell *in vivo*. The present study reported that ursolic acid (UA) strongly enhanced the antitumor action of doxorubicin (DOX) via blocking the Akt/glycogen synthase kinase-3β (Gsk3β) signaling pathway and activating tumor-suppressive Hippo signaling (mammalian Ste20-like kinase 1 and 2, salvador family WW domain containing protein 1 and MOB kinase activator 1), thereby downregulating downstream effector yes-associated protein 1 (Yap) and connective tissue growth factor (CTGF) protein expression levels in CRC cells. Furthermore, The PI3K inhibitor LY294002 further suppressed Akt activity and enhance the function of Hippo pathway-associated proteins in DOX + UA treated cells; this effect led to subsequent oncogenic Yap and CTGF inhibition following combined treatment, whereas Akt activator SC79 exerted an opposite effect in CTGF expression. *In vivo*, treatment with UA combined with DOX markedly suppressed the progression of CRC without any toxic effects on a xenograft mouse model by disrupting Akt signaling and activating the Hippo signaling pathway. These results demonstrated that UA and DOX treatment successfully induced Akt/Gsk3β inactivation via Hippo signaling pathway activation to promote Yap degradation, resulting in the inhibition of colorectal tumorigenesis. In conclusion, these findings suggested that combination therapy with UA and DOX may be more effective than DOX alone. UA may be a novel anticancer strategy and could be considered for investigation as a complementary chemotherapy agent in the future.

Introduction

Colorectal cancer (CRC) is the third most common malignancy worldwide (1,2). Morbidity due to CRC has been decreasing, primarily due to screening; however, the 5-year survival rate has not exhibited much change and the mortality rate has increased due to late diagnosis and failures in understanding the molecular pathogenesis of advanced CRC (3). Standard treatments for CRC have always been surgery, radiotherapy, immunotherapy and chemotherapy which may be used in combination to treat patients (4). Notably, more efficacious and novel approaches are required to improve the clinical outcomes in patients with CRC.

Ursolic acid (UA) is a natural product present in plants, including apples, bilberries, cranberries, elder flower, peppermint, lavender, oregano, thyme, hawthorn and prunes (5,6), which has been reported to have chemotherapeutic effects against numerous types of cancer, including CRC (7-11). UA demonstrates pharmacological properties that affect cancer development, including cytotoxic (12,13), antitumor (8,14) and anti-metastatic activity (15,16). UA has been reported

Correspondence to: Dr Soo Mi Kim, Department of Physiology, Jeonbuk National University Medical School, Gungiro 20, Deokjin, Jeonju, Jeollabuk-do 54907, Republic of Korea
E-mail: soomikim@jbnu.ac.kr

Key words: ursolic acid, doxorubicin, colorectal cancer cells, Akt, Hippo signaling pathway, yes-associated protein 1

to regulate signaling pathways, including STAT3 signaling pathway (17), TGF-β1/ZEB1 signaling pathway (18) and AMPK signaling pathway (19), to exert these antitumor effects, including inhibition of proliferation (20), promotion of apoptosis (21,22), modulation of cell cycle arrest (23,24), suppression of epithelial-to-mesenchymal transition (EMT) (8,25,26) and induction of autophagy (22,27,28). However, the precise underlying mechanisms of UA remain unknown.

Doxorubicin (DOX), an anthracycline chemotherapeutic agent, is one of the most effective chemotherapy drugs used to treat numerous types of cancer including breast, lung, gastric, ovarian, thyroid, non-Hodgkin's and Hodgkin's lymphoma, multiple myeloma, sarcoma and pediatric cancers (29-34). DOX exerts its cytotoxic activity through DNA damage by inhibiting DNA topoisomerase II and generating reactive oxygen species (32,35). DOX is the first-line anticancer agent used to treat numerous types of cancer; however, the widespread clinical use of DOX is limited by severe dose-dependent toxicity, such as renal toxicity (36), cardiotoxicity (37), hepatotoxicity (38) and neurotoxicity (39). Therefore, minimizing DOX toxicity should be considered in clinical applications.

The Hippo/yes-associated protein 1 (Yap) signaling pathway is a highly conserved adjuster of histogenesis, cell fate regulation and organ size (40), which serves essential roles in tumorigenesis, including cell proliferation, apoptosis, viability and migration (41). The core upstream units of the Hippo pathway are mammalian Ste20-like kinase (Mst) 1/2 and large tumor suppressor kinase 1/2, which form a complex that inhibits the nuclear translocation of Yap by phosphorylating Yap in the cytoplasm (42). Yap is a transcriptional co-activator that serves a crucial role in sustaining intestinal homeostasis (43). Hippo signaling pathway inactivation and Yap hyperactivation have been reported to be associated with common human malignancies, including lung cancer (44), gastric cancer (45), breast cancer (46), liver cancer (47), gliomas (48) and pancreatic cancer (49). Previous studies have demonstrated that the Hippo signaling pathway promotes stem cell properties and intestinal tumorigenesis (50-52). Mst1/2 downregulation in the intestinal epithelium has been shown to induce activation of Yap, and may contribute to tumor proliferation and metastasis (53). Moreover, the overall and disease-free survival rates of patients with CRC with Yap upregulation have been shown to be markedly decreased (54,55). There is accumulating evidence that shows that the PI3K/Akt/mTOR signaling pathway is a key survival pathway that is unconventionally activated in numerous types of malignant tumor, including CRC (56,57). Furthermore, aberrant Akt signaling pathway activation has been reported to suppress the Hippo signaling pathway, leading to increased tumorigenesis (58,59). However, the association between the Akt and Hippo signaling pathways, and its implications for the use of combined treatment with first-line chemotherapy (DOX) and a natural anticancer product (UA) remain unclear in CRC. Therefore, the present study aimed to evaluate the therapeutic effects of an anticancer herbal component-based drug in combination with chemotherapy in CRC cells.

Materials and methods

CRC cell lines and culture conditions. The human colon cancer HCT116 cell line (cat. no. 10247) and CRC HT-29 cell line (cat. no. 30038) originating from colorectal adenocarcinoma (60) were purchased from the Korean Cell Line Bank (Korean Cell Line Research Foundation) and were authenticated by Procell Life Science & Technology Co., Ltd. using STR analysis. The two cell lines were cultured in RPMI-1640 (cat. no. 23400-021; Thermo Fisher Scientific, Inc.) supplemented with 10% fetal bovine serum (cat. no. S001-07; Welgene Co., Ltd.), 1% penicillin-streptomycin (cat. no. P4333-100ml; Sigma-Aldrich; Merck KGaA) in a humidified chamber at 37˚C under 5% CO_2. UA (purity, >95%; cat. no. 10072) was purchased from Cayman Chemical Company. DOX hydrochloride (purity, 98-100%; cat. no. D1515-10MG) and SC79 (AKT activator) (purity, ≥97%; cat. no. 305834-79-1) were purchased from Sigma-Aldrich; Merck KGaA. LY294002 hydrochloride (AKT inhibitor) (purity, ≥98%; cat. no. 934389-88-5) was purchased from LKT Laboratories, Inc. Following pre-treatment with AKT inhibitor LY294002 (1 μM) for 2 h or AKT activator SC79 (5 μM) for 2 h, UA + DOX combination treatment was applied for 48 h.

Cell proliferation assay. A total of $1x10^4$ HCT116 cells or HT-29 cells were seeded onto 96-well plates and treated with DOX (500 nM, 1, 1.5, 2 μM), UA (5, 10, 15, 20 μM) or DOX (1.5 μM) with or without UA (15 μM) for 48 h at 37˚C under 5% CO_2. In the control group, no pretreatment was added. To the DMSO group, similar amounts of DMSO were added as to the DOX group (0.2 μl per well). In the combination group, DOX (1.5 μM) and UA (15 μM) were administered simultaneously. Subsequently, 10 μl EZ-Cytox (DoGenBio Co., Ltd.) was added and incubated for 2 h at 37˚C. Finally, the absorbance at 450 nm was assessed using a microplate reader (Epoch Microplate Spectrophotometer; BioTek Instruments, Inc.; cat. no. VT 05404). Cell proliferation is presented as the percentage relative to untreated cells (control group).

Soft agar colony formation assay. Briefly, a base layer containing 1% agar (micro agar, cat. no. M1002.1; Duchefa Biochemie B.V.) and a top layer containing 0.7% agar (Agarose SPI, cat. no. A1203.01; Duchefa Biochemie B.V.) were inoculated with $1x10^5$ cells per well. The medium, supplemented with UA (15 μM) and/or DOX (1.5 μM), was changed three times/week and 6-well plates were incubated for 14 days at 37˚C under 5% CO_2. Colonies were defined as >30 cells, were counted manually and were observed using an IX71 fluorescence microscope (Olympus).

Cell cycle and apoptosis assay. HCT116 and HT-29 cells ($2.5x10^5$) were seeded onto 6-well plates and treated for 48 h at 37˚C with UA (15 μM) and/or DOX (1.5 μM). Propidium iodide (cat. no. P4170; Sigma-Aldrich; Merck KGaA) and Annexin-V-FITC Assay kit (BD Biosciences) were used to stain the cells for 30 min at room temperature in the dark according to the manufacturer's protocols. BD Accuri C6 Flow Cytometer (BD Biosciences) was used to assess the cell apoptosis. Acquisition and analysis of the data were performed using BD Accuri CFlow software (version, 1.023.1; BD Biosciences). Cells that were considered viable were FITC Annexin V and PI negative; cells that were in early apoptosis were FITC Annexin V positive and PI negative; and cells that were in late apoptosis or already dead were both FITC Annexin V and PI positive.

Wound healing assay. HCT116 and HT-29 cells ($2x10^6$) were seeded onto a 6-well plate with RPMI-1640 containing 10% FBS. In order to reduce the risk of cell proliferation, 90-100% confluent HCT116 or HT-29 monolayers were incubated with RPMI-1640 containing 1% FBS, the DNA synthesis inhibitor mitomycin C (5 μg/ml) (cat. no. 10107409001; Sigma-Aldrich; Merck KGaA) 6 h prior to the scratch assay (61-63). A 200-μl pipette tip was used to scrape a straight line and cells were treated with UA (15 μM) and/or DOX (1.5 μM) for 48 h at 37˚C. The wound width in five random views was quantified at 0, 24 and 48 h to assess the effect of UA (15 μM) and/or DOX (1.5 μM) on cell migration. Images were captured with an IX71 inverted fluorescence microscope (Olympus Corporation). Migration was calculated as follows: Migration (%)=[(0 h mean scratch distance -24 or 48 h mean scratch distance)/0 h mean scratch distance] x100. The mean scratch distance can be calculated between the scratches in each of the five random views. The cell migration rate was assessed using Image-Pro Plus 6.0 software (Media Cybernetics, Inc.).

Western blotting. Western blot analysis was performed as described previously (64). Briefly, proteins were extracted from HCT116 cells, HT-29 cells and animal tumor tissues using RIPA lysis and extraction buffer containing protease and phosphatase inhibitors (Intron Biotechnology, Inc.). The supernatant was centrifuged at 16,100 x g for 30 min at 4˚C. After centrifugation, protein quantification was performed using Pierce™ Rapid Gold BCA Protein Assay kit (cat. no. A53225; Thermo Fisher Scientific Inc.). The standard curve was used to determine the protein concentration of each sample. An equal amount of total protein (30 μg/lane), and 10 μl DokDo-MARK Broad-Range Protein Ladder (cat. no. EBM-1032; ELPIS-BIOTECH, Inc.) or 10 μl Enhanced 3-color High Range Protein Marker (cat. no. PM2610; SMOBIO Technology, Inc.), were separated by SDS-PAGE on 8 and 10% gels and transferred onto 0.45 μm PVDF membranes (cat. no. 1620174; Bio-Rad Laboratories, Inc.). The membranes were blocked using 5% skimmed milk in TBS -0.1% Tween-20 (cat. no. 9005-64-5; Sigma-Aldrich; Merck KGaA) for 1 h at room temperature. The membranes were then incubated overnight at 4˚C with primary antibodies purchased from Cell Signaling Technology, Inc. as follows: GAPDH (1:1,000; cat. no. 2118S), cleaved-poly (ADP-ribose) polymerase 1 (PARP; 1:1,000; cat. no. 9541S), cleaved caspase-9 (1:1,000; cat. no. 9501S), PARP (1:1,000; cat. no. 9542S), caspase-9 (1:1,000; cat. no. 9502S), E-cadherin (1:1,000; cat. no. 5296S), cyclin D1 (1:1,000; cat. no. 2922), cyclin-dependent kinase (CDK) 4 (1,000; cat. no. 2906), CDK6 (1,000; cat. no. 3136s), Akt (1:1,000; cat. no. 9272), phosphorylated (p)-Akt (1:1,000; cat. no. 9271S), Gsk3β (1:1,000; cat. no. 12456S), p-Gsk3β (1:1,000; cat. no. 9322S), Mst1 (1:1,000; cat. no. 3682S), Mst2 (1:1,000; cat. no. 3952S), salvador family WW domain containing protein 1 (Savl; 1:1,000; cat. no. 3507), MOB kinase activator 1 (Mob1; 1:1,000; cat. no. 3863S), p-Mob1 (1:1,000; cat. no. 8699), Yap (1:1,000; cat. no. 4912) and p-Yap (1:1,000; cat. no. 4911S). Primary antibodies against Ras association domain family member 1 (Rassf1A; 1:1,000; cat. no. sc-58470), urokinase-type plasminogen activator (uPA; 1:1,000; cat. no. sc-14019), matrix metallopeptidase 9 (MMP-9; 1:1,000; cat. no. sc-6840), c-Myc (1:1,000; cat. no. sc-40) and connective tissue growth factor (CTGF; 1:1,000; cat. no. sc-14939) were purchased from Santa Cruz Biotechnology, Inc. Membranes were then incubated with anti-mouse (1:2,000; cat. no. 7076; Cell Signaling Technology, Inc.), anti-goat (1:2,000; cat. no. AF109; Novus Biologicals, Inc.) or anti-rabbit (1:2,000; cat. no. 7074S; Cell Signaling Technology, Inc.) horseradish peroxidase-conjugated secondary antibodies for >2 h at 4˚C. The enhanced HRP substrate luminol reagent was used to visualize the bands (Amersham; Cytiva). Immunoreactivity was detected using Fusion Fx7 (Vilbe, Lourmat). Films were exposed at multiple time points to ensure images were not saturated. ImageJ (version 1.52; National Institutes of Health) was used to semi-quantify the blot images.

Establishment of a HCT116 xenograft model. The animal experiments were approved by the Institutional Animal Care and Use Committee of Jeonbuk National University (approval no. CBNU2017-0001; Jeonju, South Korea) under National Institutes of Health guidelines (65). The present study was performed in compliance with the Animal Research: Reporting of *In Vivo* Experiments guidelines 2.0 (66). The present study was performed according to the guidelines on the welfare and use of animals in cancer research (67). Male SPF/BALB/c nu/nu immunodeficient mice were purchased from Orient Bio Inc. Athymic nude mice (age, 4 weeks; weight, 20±3 g; n=20) were acclimated to the animal housing conditions for 1 week. Mice were housed in an experimental animal facility under standard laboratory conditions (20-25˚C, 40-60% humidity, 12-h light/dark cycle) with free access to food and water. HCT116 cells ($1x10^7$) in 100 μl Matrigel (Corning Matrigel Basement Membrane Matrix; cat. no. 356234; Corning, Inc.) were injected into the flank area of the mice. After inoculation, HCT116 tumor-bearing animals were assigned to four groups (n=5/group) as follows: i) vehicle; ii) UA; iii) DOX; and iv) UA + DOX and housed in individually ventilated cages with litter and nesting material. The mice in the vehicle group were administered 20 μl sterile DMSO twice weekly. The mice in the UA group were treated with 10 mg/kg/day UA in 100 μl PBS. The mice in the DOX group were administered 2 mg/kg DOX in 20 μl DMSO twice weekly. The mice in the DOX + UA combination group were administered 2 mg/kg DOX in 20 μl DMSO twice weekly and 10 mg/kg/day UA in 100 μl PBS. All agents were administered via intraperitoneal injection. The average volume of the tumors was calculated as follows: Tumor volume=$width^2$ x length/2. The body weight of mice was monitored every 2 days. Mouse welfare was assessed daily and palpable tumors were assessed every other day. All mice could reach food and water, and all had a fairly normal gait. Mice moved freely in the cage with normal body and tail position and in a forward motion; the abdomen of the mice was soft with a mild resistance to pressure when touched and abdominal distention was not observed in the mice following injection of the drugs. All mice demonstrated a slightly curved back and did not have a hunched position when sitting or during rest. One mouse had bite wounds on the tail and back; however, blood stains were absent in the cage and the mouse was separated to an individual cage on day 13. Wounds were locally disinfected daily until healed and the mouse was isolated until the end of the procedure.

All mice had no ocular or nasal discharge. When the skin of the neck of the mice was pinched, one mouse in the control group demonstrated poor skin turgor and the tumor diameter of this mouse reached 2 cm on day 22. The poor turgor indicated that this mouse was dehydrated and all mice were sacrificed on day 22. Mice were placed in a chamber with 4% isoflurane (cat. no. 1349003; Sigma-Aldrich; Merck KGaA) until animals lost consciousness and CO_2 (50% of the chamber vol/min) was used to euthanize the mice. Death was confirmed by loss of heartbeat, toe reflex, muscle tone, breathing and corneal reflex, and rigor mortis; subsequently, tumor tissues were harvested.

Assessment of serum biochemical biomarkers. Serum concentrations of aspartate aminotransferase (AST; cat. no. 10103; Asan Pharmaceuticals Co., Ltd.), alanine aminotransferase (ALT; cat. no. 10102; Asan Pharmaceuticals Co., Ltd.), blood urea nitrogen (BUN; cat. no. K024-H1; Arbor Assays LLC Co., Ltd.) and creatinine (cat. no. KB02-H1; Arbor Assays LLC Co., Ltd.) were determined using commercial kits.

Histopathology and immunohistochemistry staining. At the end of the animal experiment, mouse tumor tissue samples were embedded in 10% formaldehyde at 4˚C for 24 h, sliced into 4-μm sections and stained using hematoxylin and eosin (H&E) following a standard protocol for histopathological examination (68). For immunohistochemistry staining, sections from mouse tumor tissue were prepared according to the manufacturer's protocol using the Rabbit HRP/DAB Detection IHC kit (cat. no. ab64261; Abcam). Samples were deparaffinized with xylene, rehydrated with a descending ethanol series l (100, 95, 90, 80 and 70% ethanol) at room temperature for 5 min and subjected to antigen retrieval by boiling samples in decreasing concentrations of EDTA buffer (pH 9.0) at 120˚C for 2 min, followed by cooling to room temperature for 30 min. Slides were blocked using hydrogen peroxide blocking buffer (supplied in the kit) for 15 min to quench endogenous peroxidase and 10% goat serum (cat. no. 16210064; Thermo Fisher Scientific, Inc.) at room temperature for 30 min each. Slides were washed with PBS and incubated with rabbit anti-Ki-67 (1:100; cat. no. PA5-16785; Invitrogen; Thermo Fisher Scientific, Inc.) primary antibodies overnight at 4˚C and biotinylated goat anti-rabbit IgG and streptavidin peroxidase (cat. no. ab64261; Abcam) at room temperature for 2 h. Slides were washed with PBS and counterstaining was performed using 100 μl diaminobenzidine at room temperature for 1 min and sufficient hematoxylin to cover the slides at room temperature for 1 min. Histopathological assessment and immunohistochemistry staining analysis were performed using a light microscope.

Statistical analysis. *In vitro* experiments were performed in triplicate. The number used for animal experiments was n=5. Data analysis was performed using GraphPad Prism 8 software (GraphPad Software, Inc.). One-way ANOVA followed by Tukey's post hoc test was used to assess differences among ≥3 groups. The data are presented as the mean ± SEM. $P<0.05$ was considered to indicate a statistically significant difference.

Results

UA enhances DOX-mediated inhibition of CRC cell proliferation. In the present study, the anti-proliferative effects of UA and DOX were assessed by cell proliferation assay to evaluate cytotoxicity. The UA and DOX concentrations used in the *in vitro* experiments were based on the cell proliferation assay results. Following 48 h of exposure, UA or DOX markedly inhibited the cell proliferation of both HCT116 and HT29 cells in a concentration-dependent manner compared with the control (Fig. S1). DOX (1.5 μM) treatment of HCT116 cells caused significant cell proliferation suppression compared with in the control group (Fig. 1A). The UA (15 μM) + DOX (1.5 μM) combination treatment significantly inhibited cell proliferation compared with in the UA and DOX groups. HT-29 cell proliferation was significantly decreased (75-85% after 48 h) by co-treatment compared with either agent alone. These data suggested that cell proliferation was significantly suppressed by the combination of UA + DOX compared with either agent alone. Subsequently, a soft agar colony formation assay was performed using CRC cells to assess the effect of combination treatment on colony formation. UA + DOX markedly decreased the size and significantly decreased the number of colonies compared with each drug alone in both CRC cell lines (Fig. 1B).

UA enhances DOX-induced CRC cell apoptosis. Flow cytometry was used to assess the apoptotic status of cells following treatment with different drugs. It has been reported that the sub-G_1 phase is characterized by apoptosis induction (69). The proportion of cells in sub-G_1 phase was significantly increased following treatment with the combination of 15 μM UA + 1.5 μM DOX compared with the control and either agent alone (Figs. 1C and S2A). PI/FITC assay results demonstrated that the combination treatment significantly induced apoptosis compared with the control and either agent alone (Fig. 1D). Furthermore, western blotting demonstrated markedly decreased caspase-9, significantly decreased PARP, and significantly increased cleaved caspase-9/caspase-9 and cleaved-PARP/PARP protein expression levels following treatment with the combination of 15 μM UA + 1.5 μM DOX compared with the single treatments in HCT116 and HT-29 cells (Fig. 1E). These data were consistent with the flow cytometry results. The present study indicated that combination treatment triggered the apoptosis of CRC cells.

UA enhances DOX-mediated suppression of CRC cell migration via EMT signaling pathway inhibition. Distant cancer cell metastasis is a key step that includes migration, invasion and EMT, which represents an advanced malignancy stage (70). The migratory ability of CRC cells, as demonstrated using wound healing assay, was significantly decreased following treatment with the combination of UA + DOX compared with UA or DOX alone (Fig. 2A). Investigation of EMT-associated regulators was performed using western blotting. The protein expression levels of E-cadherin, an epithelial marker, were markedly increased, whereas the protein expression levels of mesenchymal markers (MMP-9 and uPA) were significantly decreased in the combination groups in both cell lines compared with the control and either agent alone

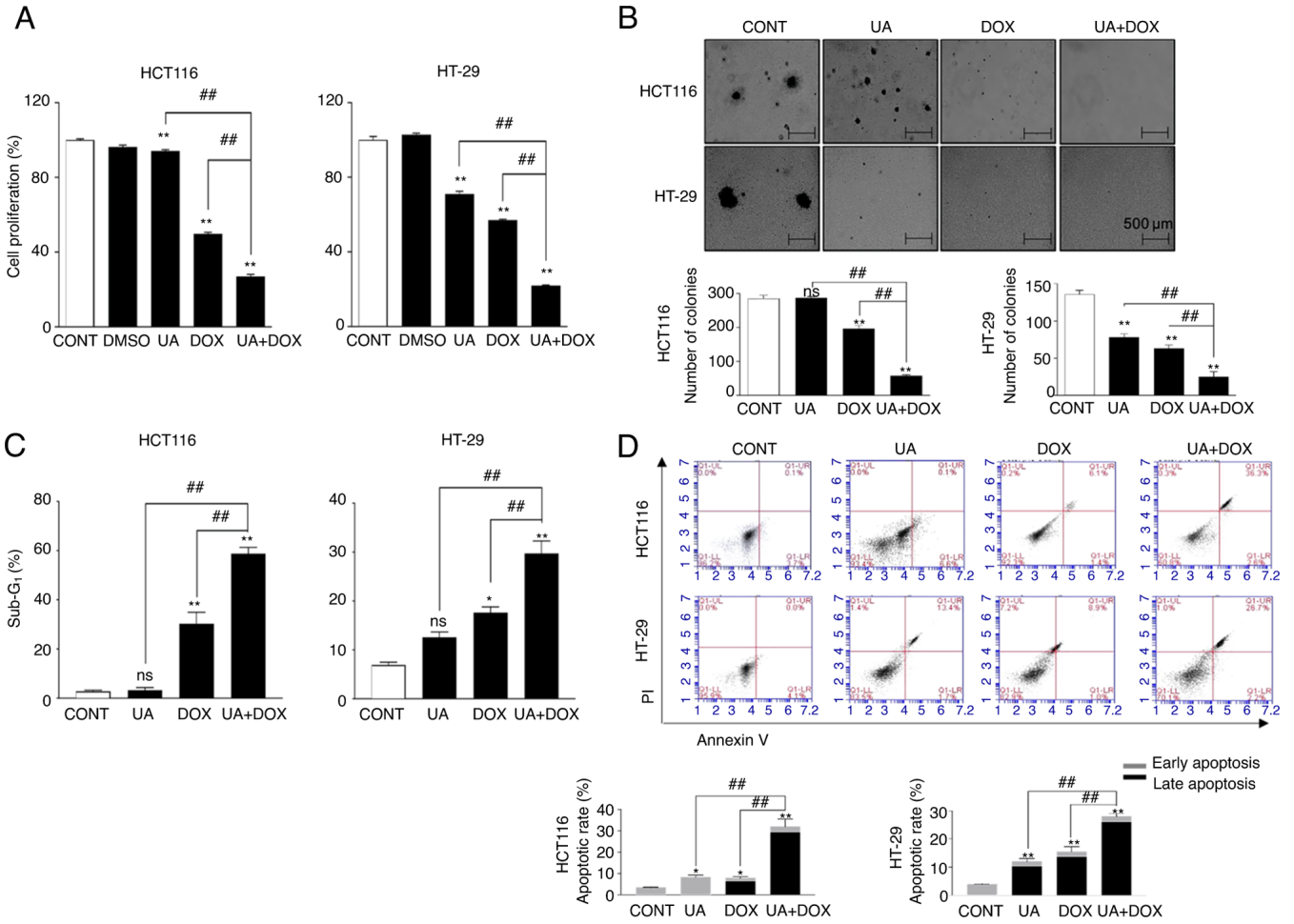

Figure 1. Continued.

(Fig. 2B). These data demonstrated that combination treatment with UA + DOX may have inhibited cell migration via disruption of the EMT process.

Combination treatment with UA + DOX increases the proportion of CRC cells in G_1 phase. In the present study, flow cytometry was used to assess cell cycle progression. The results suggested that UA did not affect G_1 phase in HCT116 and HT29 cell lines, whereas cell accumulation in G_1 phase was markedly increased following DOX treatment compared with in the control group. Furthermore, combination treatment with UA + DOX in HCT116 and HT-29 cells further induced G_1 phase arrest, followed by a marked decrease in the number of cells in G_2 phase compared with in the control group (Figs. 3A and S2B). Western blotting demonstrated that cyclin-dependent kinase (CDK)4/6 and cyclin D1 protein expression levels, which are essential for DNA synthesis (71), were significantly downregulated following combination treatment compared with in the control group (Fig. 3B). Collectively, these data indicated that UA further enhanced DOX-mediated cell cycle arrest in the G1 phase in HCT116 and HT-29 cell lines.

UA enhances DOX-mediated downregulation of Akt signaling pathway-associated proteins in CRC cells. Growing evidence has indicated that overactive PI3K/Akt signaling serves a crucial role in cell migration and proliferation, as well as apoptosis inhibition (72-74). In the present study, the protein expression levels of p-Akt, p-Gsk3β and c-Myc were assessed using western blotting to evaluate the effects of UA and DOX treatment on the Akt signaling pathway. The combination treatment of UA + DOX significantly decreased the protein expression levels of p-Akt and c-Myc, which is downstream of the Akt signaling pathway (75), compared with the control, whereas the total level of Akt remained unchanged (Fig. 4). Consistently, p-Gsk3β (S9) expression levels were markedly decreased by combination treatment compared with UA or DOX alone (Fig. 4). Collectively, these results demonstrated that combination treatment with UA + DOX exerted anticancer effects by inhibiting the Akt signaling pathway.

UA enhances DOX-mediated activation of the Hippo pathway in CRC cells. Guo *et al* (76) reported that Rassf1A directly binds to Mst1 and Mst2, inhibiting tumorigenesis by activating the Hippo signaling pathway. Therefore, the effect of combined treatment on the expression levels of Rassf1A and Hippo signaling pathway-associated proteins were assessed using western blotting. Mst1 and Mst2 activate downstream tumor suppressor Sav1, which also serves a key role in the Hippo pathway (77). The expression levels of Rassf1A, Mst1/2, Sav1 and the ratio of p-Mob1/Mob1 were

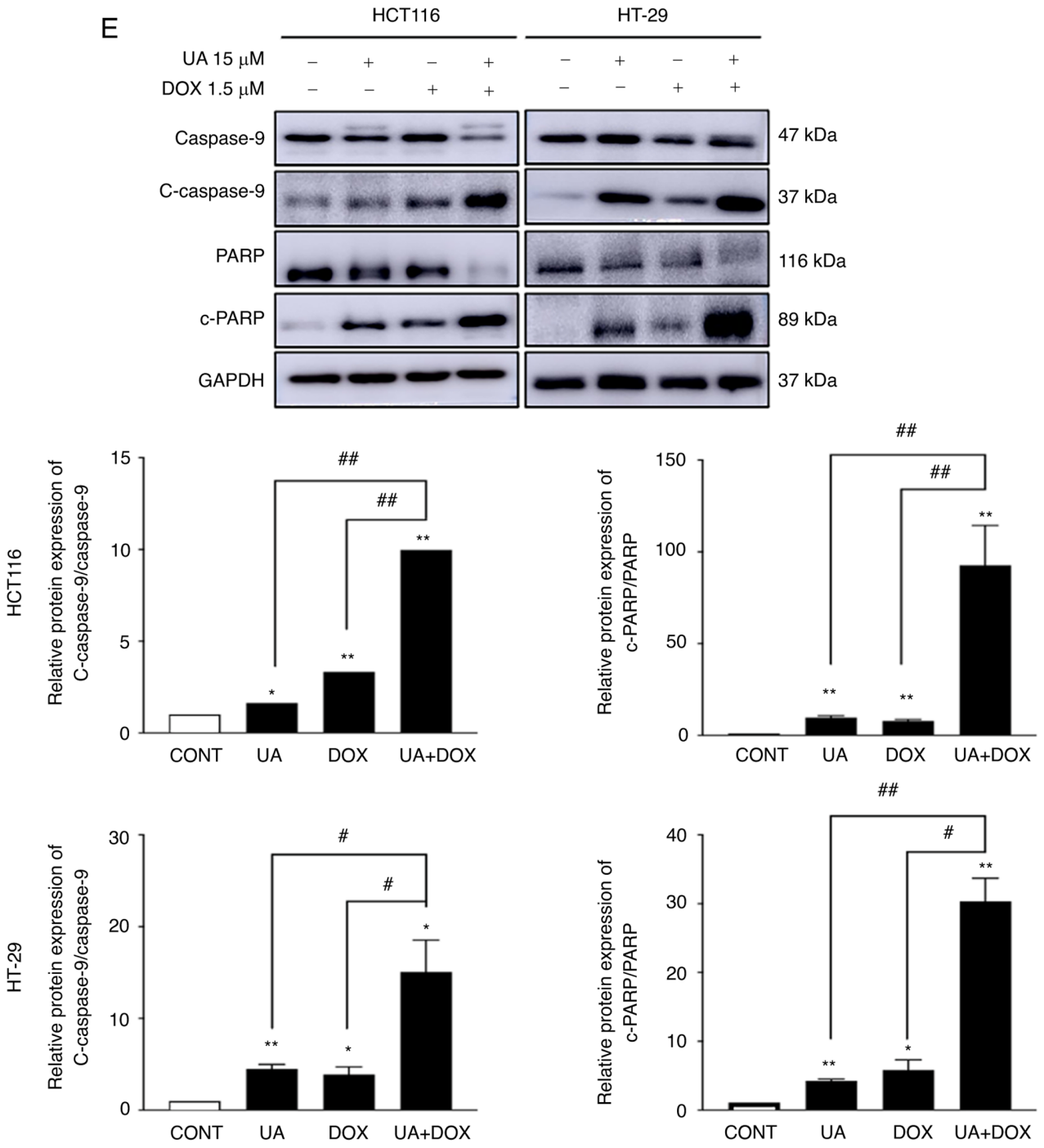

Figure 1. Effect of UA and DOX on the proliferation, colony formation and apoptosis of HCT116 and HT-29 CRC cells. (A) Human CRC cells in logarithmic growth phase were treated with UA (15 μM) and DOX (1.5 μM) for 48 h. Inhibitory effects on cell proliferation were assessed using cell proliferation assay. (B) Colony formation assay. UA + DOX significantly inhibited colony formation in colon cancer cells compared with the control after 2 weeks. (C) Proportion of cells in sub-G_1 phase increased following treatment with UA + DOX. (D) HCT116 and HT-29 cells were collected to assess apoptotic rate using FITC/PI double-positive staining following UA + DOX treatment. (E) Following CRC cell treatment with UA (15 μM) or DOX (1.5 μM) for 48 h, apoptosis-associated c-PARP, PARP, c-Caspase-9 and Caspase-9 expression was semi-quantified using western blotting. Values were normalized to GAPDH. *P<0.05, **P<0.01 vs. control; $^{\#}$P<0.05, $^{\#\#}$P<0.01. vs. UA/DOX.. Scale bar, 500 μm. CONT, control; DMSO, dimethyl sulfoxide; UA, ursolic acid; DOX, doxorubicin; CRC, colorectal cancer; PARP, poly (ADP-ribose) polymerase 1; PI, propidium iodide; ns, not significant; c-, cleaved.

all significantly elevated following combination treatment compared with UA or DOX treatment alone in both CRC cell lines (Fig. 5A and E). Furthermore, the protein expression levels of p-Yap, which is the inactivated form of Yap, were significantly induced by combined treatment compared with the control. However, Yap protein expression levels were significantly decreased compared with the control. Furthermore, combination treatment significantly suppressed the protein expression levels of CTGF, which is a target of Yap (78), compared with the control (Fig. 5B and F). Collectively, these results indicated that UA + DOX combined treatment may inhibit Yap-induced CRC progression by activating the Hippo signaling pathway. Subsequently, the effects of an Akt inhibitor (LY294002) and activator (SC79)

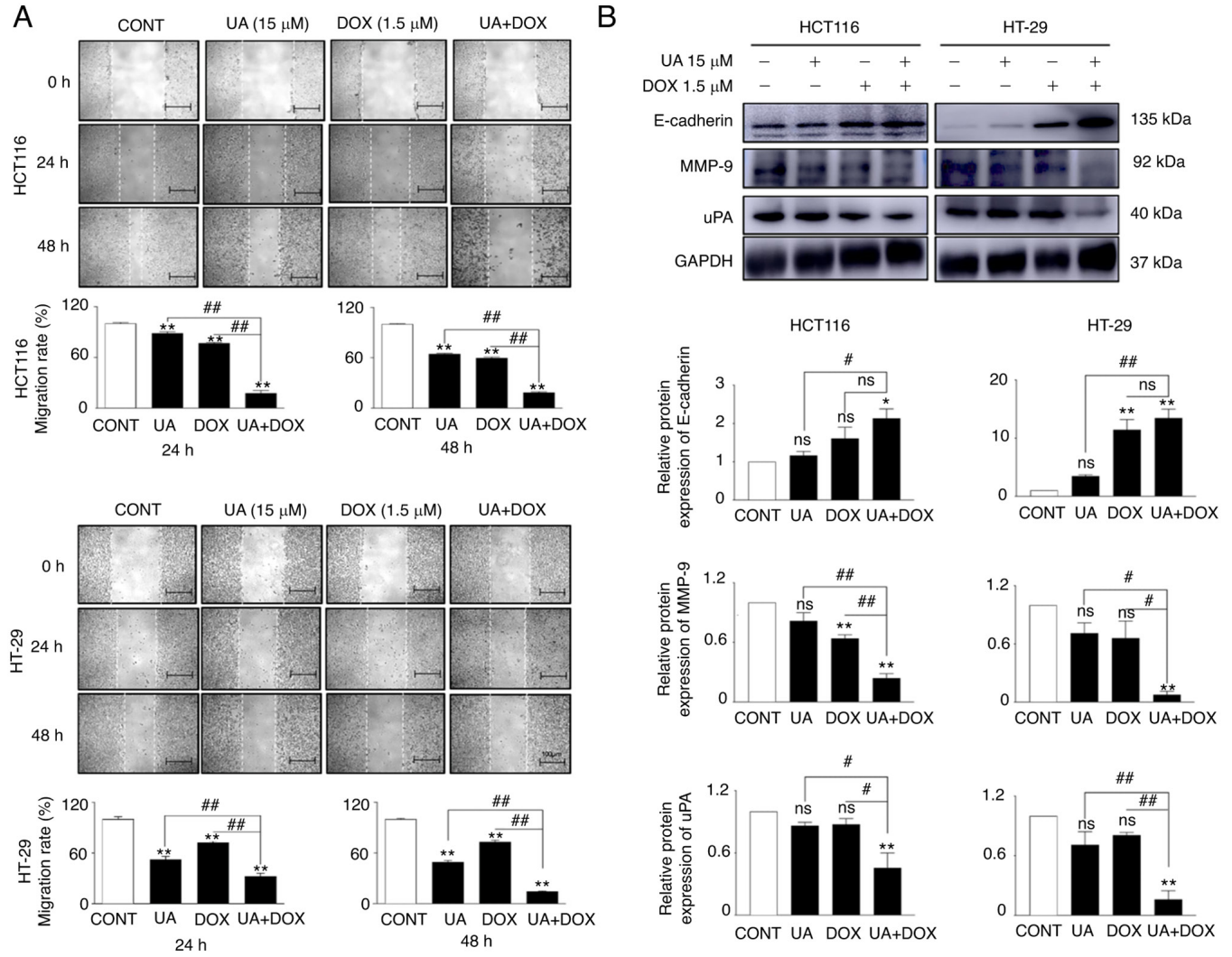

Figure 2. Effects of UA and DOX on migration and the EMT pathway in HCT116 and HT-29 CRC cells. (A) Migration of CRC cells was assessed using a wound healing assay following treatment with 15 μM UA or 1.5 μM DOX or a combination. The cell migration ability was significantly inhibited when treated with the combination at 24 and 48 h. (B) Western blotting was used to semi-quantify EMT pathway-associated protein expression levels of E-cadherin, uPA and MMP-9 following UA and DOX treatment for 48 h in HCT116 and HT-29 CRC cells. Values were normalized to GAPDH. *P<0.05, **P<0.01 vs. control, $^{\#}$P<0.05, $^{\#\#}$P<0.01. vs. UA/DOX. CONT, control; UA, ursolic acid; DOX, doxorubicin; MMP-9, matrix metallopeptidase-9; uPA, urokinase-type plasminogen activator; ns, not significant; EMT, epithelial-to-mesenchymal transition.

on the Hippo pathway were assessed to evaluate the crosstalk between the Hippo and Akt pathways. LY294002, a PI3K inhibitor, restricts downstream Akt signaling activity (79). LY294002 markedly decreased the ratio of p-Akt/Akt while activating the Hippo pathway compared with control group (Fig. 5C and G). The expression levels of Hippo pathway proteins Rassf1A, Mst1 and Sav1 demonstrated no significant difference following SC79 treatment. Notably, combination treatment of LY294002 + UA + DOX significantly inactivated Akt signaling activity as demonstrated by significantly increased protein expression levels of Rassf1A, Mst1/2 and Sav1 compared with the UA + DOX treatment group. LY294002 + UA + DOX treatment also enhanced the expression of p-Yap while significantly increasing the ratio of p-Yap/Yap and decreasing the expression of its target CTGF (Fig. 5D and H). Collectively, these results demonstrated that combination treatment of LY 294002 + UA + DOX resulted in the inhibition of Akt activity together with Hippo signaling pathway activation.

UA enhances DOX-mediated antitumor activity in an HCT116 xenograft mouse model. Based on the aforementioned *in vitro* data, the anti-CRC effects of UA and DOX were evaluated in xenograft tumor tissue *in vivo*. A concentration of 15 μM UA was used to assess whether a low concentration of UA enhanced the action of DOX. DOX concentration was selected using half maximal inhibitory concentration values (data not shown). The data from *in vitro* experiments suggested that cell proliferation was significantly suppressed by the combination of 15 μM UA + 1.5 μM DOX compared with UA or DOX treatment alone. Certain previous studies reported that administration of UA (12.5 mg/kg daily) or UA (10 mg/kg for 5 consecutive days) significantly inhibited tumor growth in CRC xenograft mouse models (80,81). Our previous study also demonstrated that UA treatment (10 mg/kg daily) suppressed tumor growth in an esophageal cancer xenograft mouse model, and did not impair liver or kidney function (64). Other previous studies have reported that DOX (2 mg/kg/week) or DOX (5 mg/kg every 2 days for a total of five times) treatment

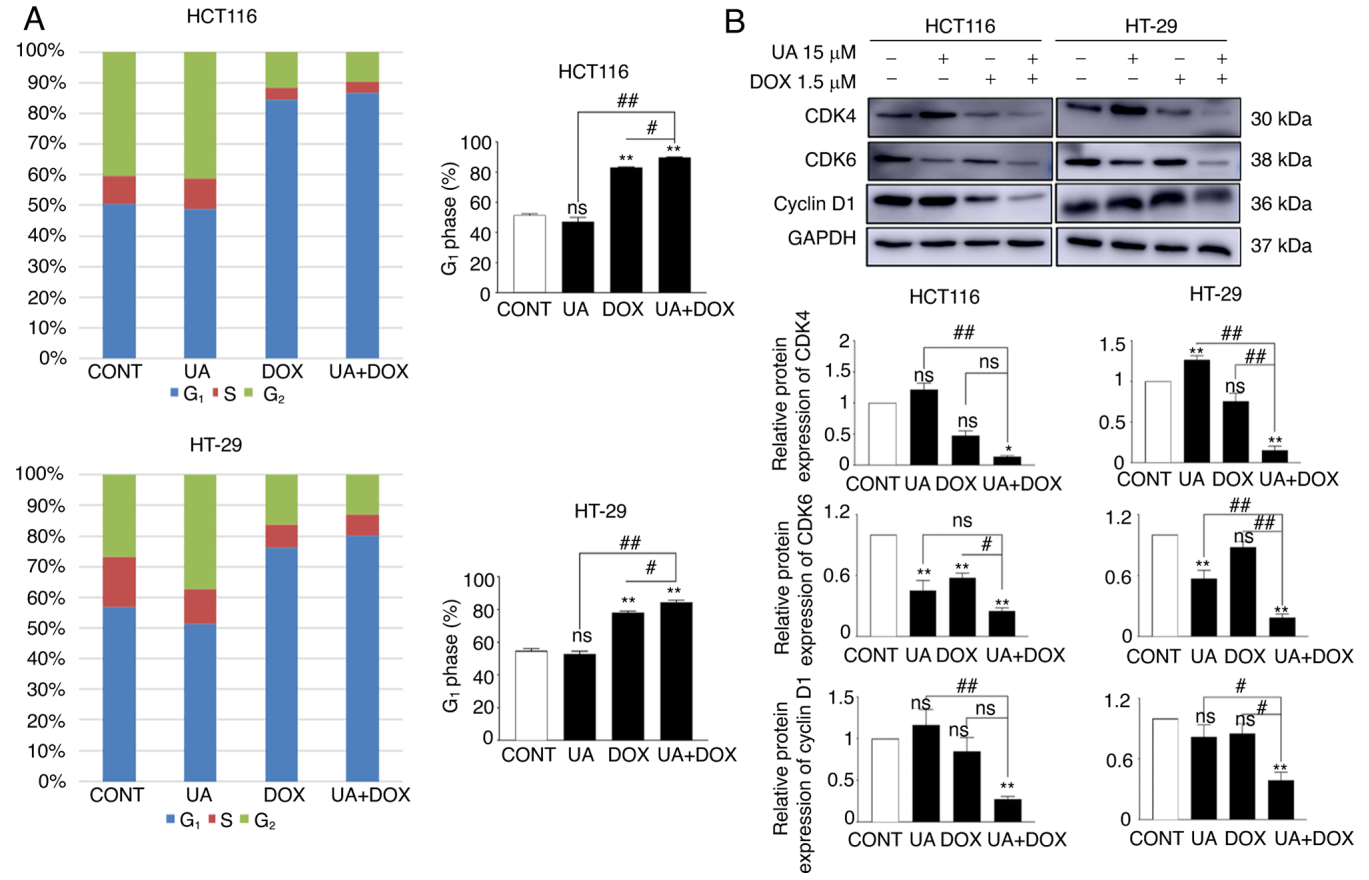

Figure 3. Effect of UA and DOX on cell cycle distribution in HCT116 and HT-29 CRC cells. (A) UA and DOX were applied to CRC cells to assess cell cycle distribution. (B) Cell cycle-associated protein (CDK and cyclin D1) levels were assessed by western blotting following combination treatment for 48 h in the HCT116 and HT-29 cell lines. Values were normalized to GAPDH. *P<0.05, **P<0.01 vs. control, $^{\#}$P<0.05, $^{\#\#}$P<0.01. vs. UA/DOX. CONT, control; UA, ursolic acid; DOX, doxorubicin; CRC, colorectal cancer; CDK, cyclin-dependent kinase; ns, not significant.

suppressed mouse CRC xenografts *in vivo* (82,83). Therefore, based on the concentration used in other studies, experimental dosages of 10 mg/kg UA for 5 consecutive days and 2 mg/kg DOX twice a week were selected for the CRC xenograft mouse model. Previous studies have recommended human DOX dosage to be 60-75 mg/m^2 as a single intravenous injection administered at 21-day intervals, with a lifetime cumulative dose limit of 550 mg DOX/m^2 body surface area (84,85). For body surface normalization, human values were corrected for the mean body surface area of 1.62 m^2 (60 kg) and mouse values were corrected for the mean body surface area of 0.07 m^2 (20 g) (86). Therefore, the mouse equivalent dose was determined using the following equation: Mouse equivalent dose (mg/kg)=human dose (mg/kg) x (human K_m/mouse K_m) where the K_m factor for each species was constant [human K_m, 37; mouse K_m, 3; K_m is estimated by dividing the average body weight (kg) of species to its body surface area (m^2)] (87). Based on recommended human DOX dosage, the mouse equivalent dose was 19.98-24.975 mg/kg. In the present study, low dose DOX (2 mg/kg, twice/week) treatment with a cumulative dose of <10 mg/kg notably inhibited tumor growth in the CRC xenograft mice model (data not shown).

In the present study, levels of the biochemical markers ALT, AST, BUN and creatinine were assessed in mouse serum to evaluate the organ toxicity of UA and DOX. UA and DOX treatment did not significantly affect the ALT, AST, BUN or creatinine level between the four groups (Fig. 6A-D). This result indicated that the doses of UA and DOX did not impair liver or kidney function. As presented in Fig. 6E, the weight of most of the tumor-bearing mice remained unchanged throughout the study period, with only three mice losing <5% of their weight in the vehicle and UA treatment groups. UA and DOX treatment alone significantly decreased tumor weight (Fig. 6F), tumor size (Fig. 6G) and tumor volume (Fig. 6H) compared with in the vehicle group. UA and DOX treatment demonstrated notable inhibition of tumor growth compared with the control group in the xenograft model. Furthermore, a marked different histology was demonstrated using H&E staining (Fig. 6I). Aggressive tumor cell proliferation with a high nucleus/cytoplasm ratio was observed in the control group, whereas the combination of UA + DOX treatment induced lymphocyte infiltration around tumor cells and increased the areas of apoptosis (Fig. 6I). Moreover, immunohistochemistry staining demonstrated that expression of the proliferation marker Ki-67 in the UA + DOX treatment group was lower than that in the control group, which suggested that the combination of UA + DOX suppressed tumor growth and development *in vivo*. Tumor samples were harvested and western blot analysis was performed to assess the molecular mechanisms underlying the effects of combination treatment *in vivo*. The combination treatment significantly decreased the p-Akt/Akt ratio compared with UA or DOX alone while

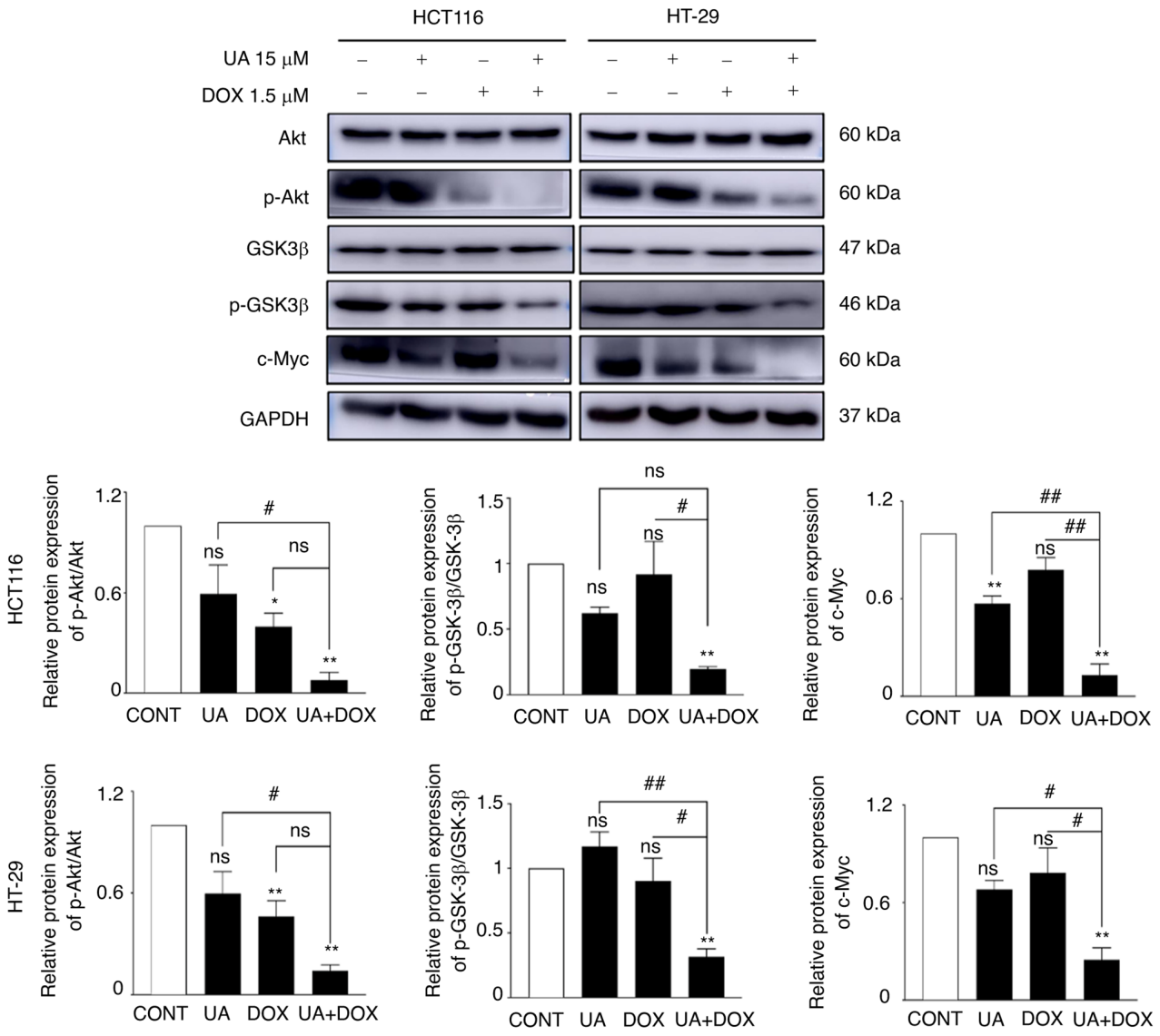

Figure 4. Effect of UA and DOX on the Akt signaling pathway. Protein expression levels of Akt, p-Akt, Gsk3β, p-Gsk3β and c-Myc was assessed using western blotting following UA, DOX or combination treatment for 48 h. Values were normalized to GAPDH. *P<0.05, **P<0.01 vs. control, $^{\#}$P<0.05, $^{\#\#}$P<0.01. vs. UA/DOX. CONT, control; UA, ursolic acid; DOX, doxorubicin; ns, not significant; p, phosphorylated; Gsk3β, glycogen synthase kinase-3β.

markedly activating the Hippo signaling pathway compared with UA or DOX alone (Fig. 6J-L). Collectively, these *in vivo* results demonstrated that UA augmented the antitumor effects of DOX via inactivation of Akt and activation of the Hippo signaling pathway in the mouse xenograft model.

Discussion

The precision of CRC diagnosis has improved in recent years; however, CRC is the fourth most commonly diagnosed and the third deadliest cancer worldwide (88). The primary biological characteristics of metastatic CRC are tumor cell proliferation and migration, and this type of cancer has limited therapeutic options and is thus associated with a higher risk of mortality (89,90). With rapid development of molecular genetic analysis of human metastatic CRC, treatments that target specific signaling pathways, including TGF-β (transforming growth factor-β)/SMAD (91), Wnt/β-catenin (92), EGFR-related pathway (93) and VEGF/VEFGR pathway (94) have been reported as a potential approach for CRC therapy (95). Studies on the anticancer efficacy of UA (96,97) or DOX (98) have been performed; however, to the best of the authors' knowledge, the effects of UA on the efficacy of DOX in human CRC cells have not been reported. The present study demonstrated that UA and DOX served a key role in the crosstalk between the Hippo and Akt signaling pathways, resulting in the inactivation of tumorigenesis in colon cancer cells.

In this study, HCT116 and HT-29 were used because HCT116 is a highly aggressive cell line with little or no capacity to differentiate, whereas HT-29 has an intermediate capacity to differentiate into enterocytes and mucin-expressing lineages. The HCT116 cell line was originally isolated from a colon primary tumor (99,100) and the HT-29 cell line originated from a colorectal adenocarcinoma (60). Ahmed *et al* (101) assessed the genetic mutation status of the HCT116 and HT-29 cell lines. It was reported that HT-29 exhibited deficient *TP53* expression, whereas HCT116 had gained a *KRAS*

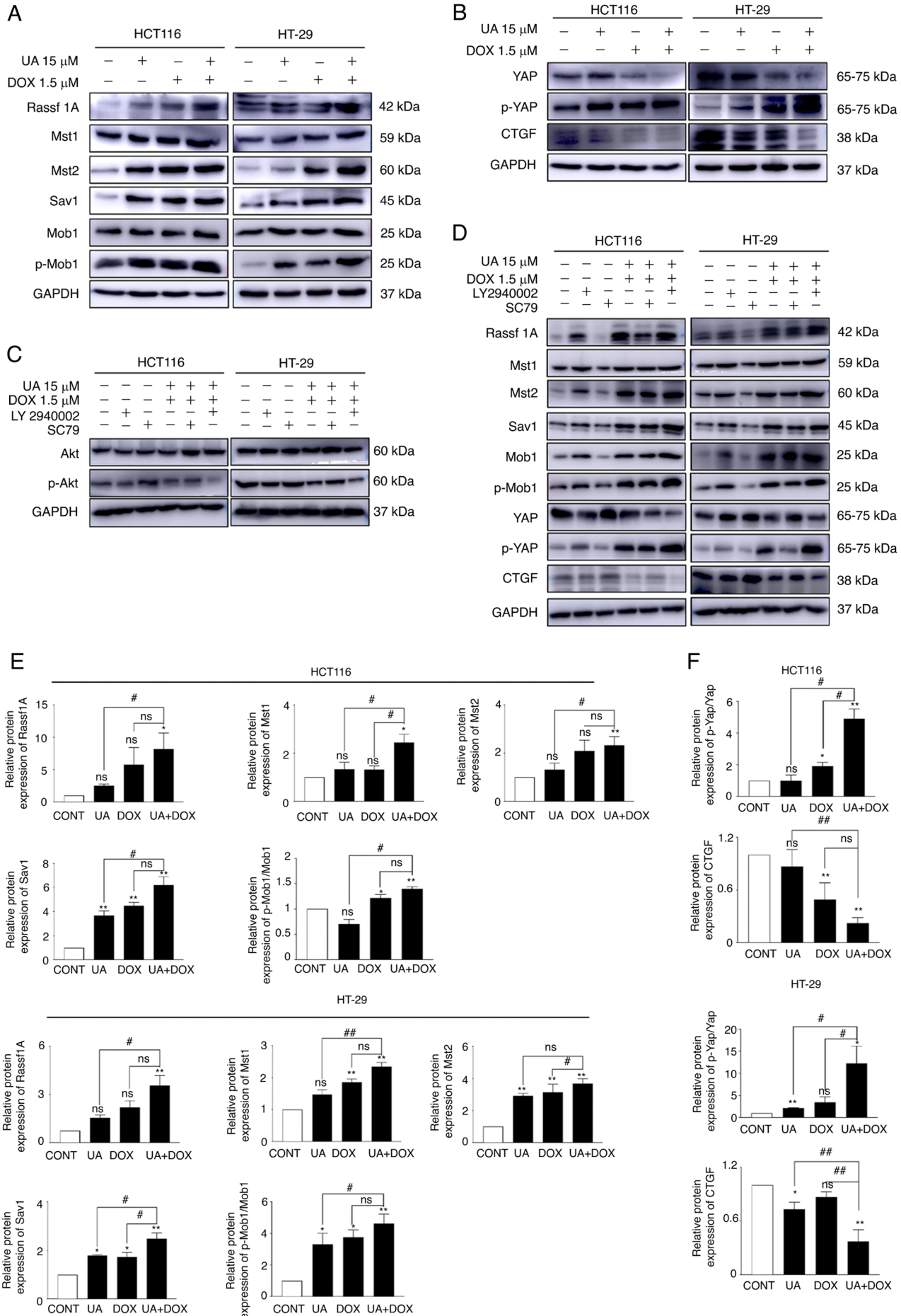

Figure 5. Continued.

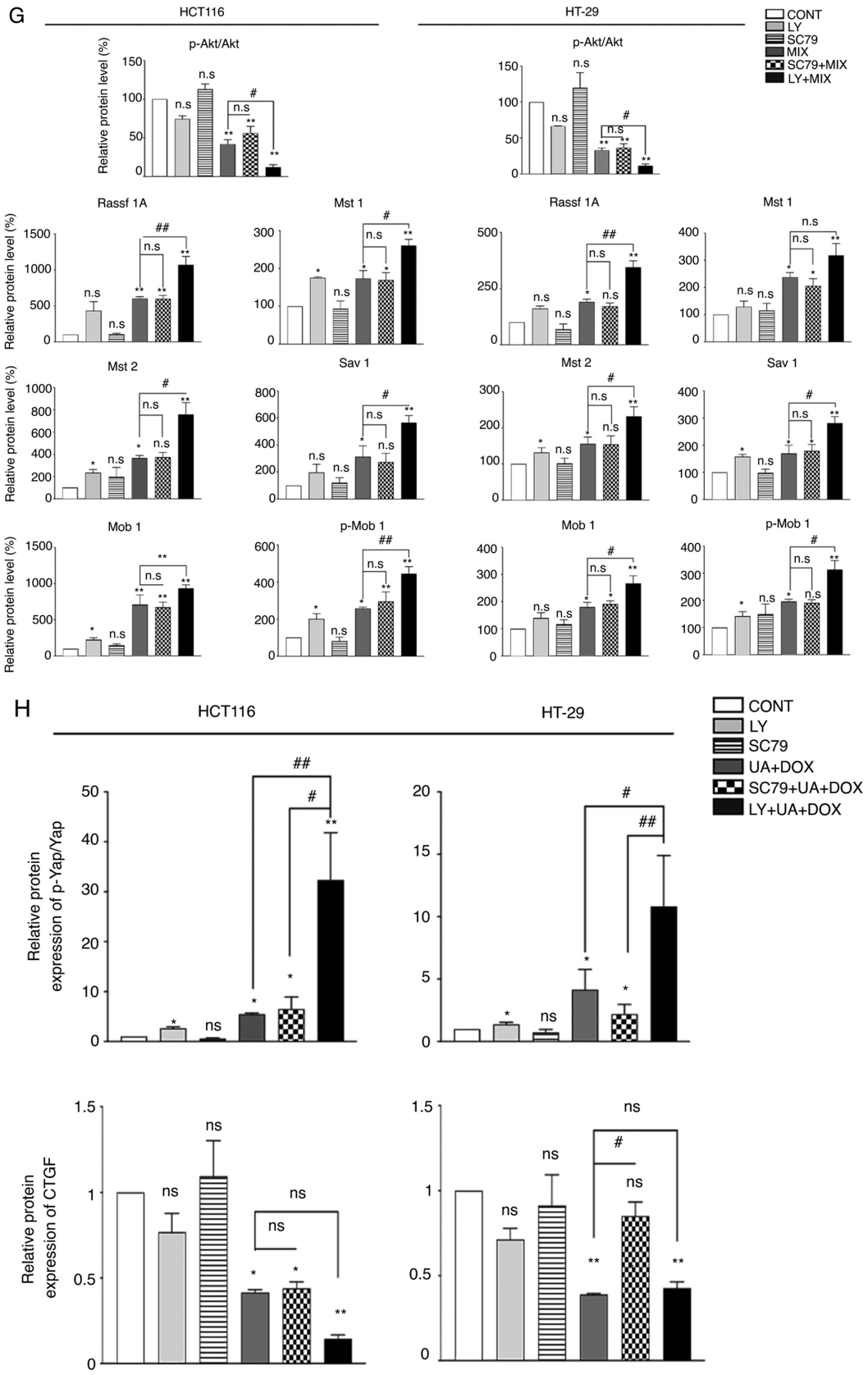

Figure 5. Expression levels of Hippo signaling pathway-associated downstream proteins following inhibition or activation of Akt expression. Expression levels of (A) Hippo pathway-associated proteins, and (B) Yap, p-YAP and CTGF were assessed by western blotting. Western blotting was performed to assess the expression levels of (C) Akt signaling pathway-associated proteins and (D) Hippo signaling pathway-associated proteins. Expression levels of Hippo pathway-associated proteins (E) Rassf1A, Mst1/2, Sav1, Mob1 and p-Mob1; and (F) Yap, p-YAP and CTGF following UA and DOX treatment were semi-quantified using ImageJ. Expression levels of (G) Akt signaling pathway-associated proteins p-Akt and Akt, Hippo signaling pathway-associated proteins Rassf1A, Mst1/2, Sav1, Mob1 and p-Mob1; and (H) Yap, p-YAP and Y CTGF following Akt activator and inhibitor, and UA and DOX treatment were semi-quantified using ImageJ. Values were normalized to GAPDH. *P<0.05, **P<0.01 vs. control, $^{\#}$P<0.05, $^{\#\#}$P<0.01. vs. UA/DOX. CONT, control; UA, ursolic acid; DOX, doxorubicin; Yap, yes-associated protein 1; Mob1, MOB kinase activator 1; Mst, mammalian Ste20-like kinases; CTGF, connective tissue growth factor; Sav1, salvador family WW domain containing protein 1; Rassf1A, Ras association domain family member 1; p, phosphorylated; ns, not significant.

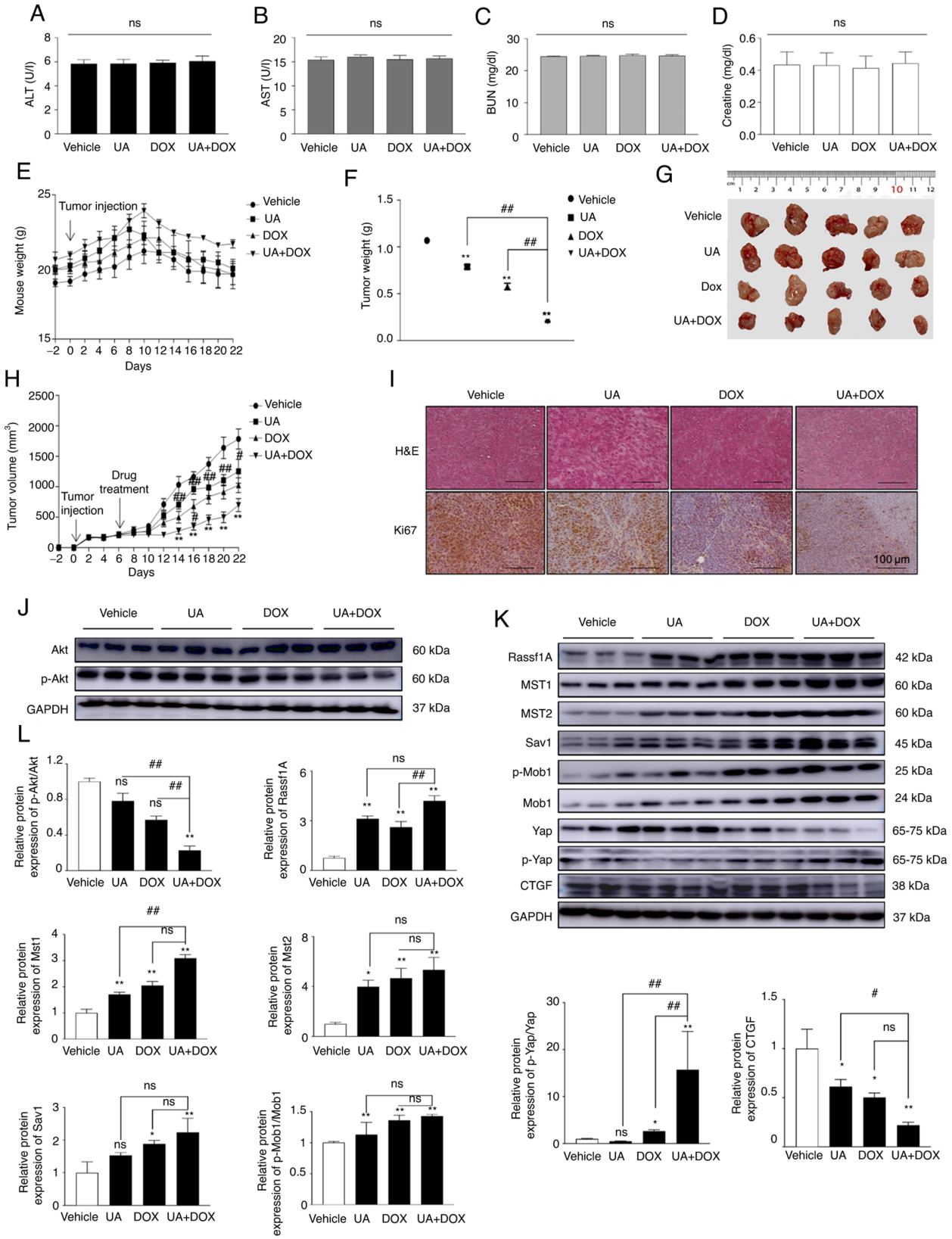

Figure 6. *In vivo* effects of UA and DOX on a HCT116 xenograft mouse model. A xenograft mouse model was established on day 0 and was treated with DMSO, UA, DOX or UA + DOX on days 6-22. On day 22, all mice were sacrificed and samples were harvested. (A) ALT, (B) AST, (C) BUN and (D) creatinine levels were assessed. (E) Body weight was assessed in tumor-bearing mice following treatment. (F) Final tumor weight and (G) representative tumor images were obtained at the end of the experiment. (H) The tumor volume was monitored every two days. (I) Tumor sections were stained using H&E and Ki-67 for immunohistochemistry analysis. (J) Western blotting was performed to assess the expression levels of Akt signaling-associated proteins in tumor tissue. (K) Western blotting was performed to assess the expression levels of Hippo signaling-associated proteins in tumor tissue. (L) The expression levels of Akt and Hippo signaling-associated proteins were semi-quantified using ImageJ. GAPDH was used as the internal control. *P<0.05, **P<0.01 vs. control, $^{\#}$P<0.05, $^{\#\#}$P<0.01. vs. UA/DOX. UA, ursolic acid; DOX, doxorubicin; H&E, hematoxylin and eosin; AST, aspartate aminotransferase; ALT, alanine aminotransferase; BUN, blood urea nitrogen; Yap, yes-associated protein 1; Mob1, MOB kinase activator 1; Mst, mammalian Ste20-like kinases; CTGF, connective tissue growth factor; Sav1, salvador family WW domain containing protein 1; Rassf1A, Ras association domain family member 1; p, phosphorylated; ns, not significant.

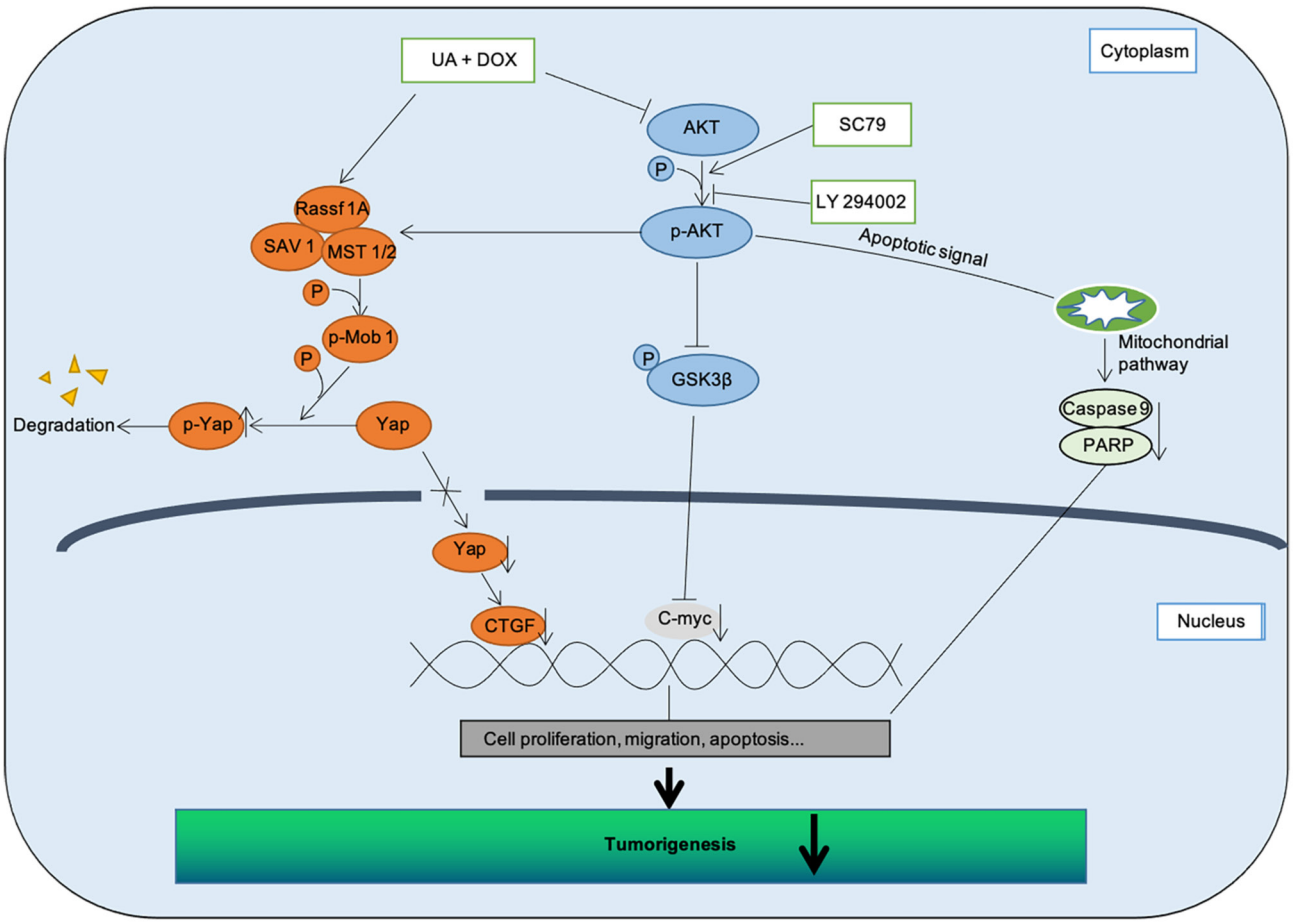

Figure 7. Schematic diagram. Combination treatment of UA + DOX results in tumorigenesis inhibition, mediated by targeting Akt/Gsk3β signaling and activating tumor-suppressive Hippo signaling, thereby inducing degradation of p-Yap in CRC cells. Combination of UA + DOX therapy reduced proliferation and promoted apoptosis in CRC cells by activating Akt-mediated effects of the mitochondrial pathway. Following combined UA + DOX treatment, LY294002 further inhibited Akt activity activating Hippo signaling pathway. Mob1, MOB kinase activator 1; Mst, mammalian Ste20-like kinases; CTGF, connective tissue growth factor; Sav1, salvador family WW domain containing protein 1; Rassf1A, Ras association domain family member 1; p, phosphorylated; Gsk3β, glycogen synthase kinase-3β; PARP, poly(ADP-ribose) polymerase 1; UA, ursolic acid; DOX, doxorubicin.

mutation (101), which resulted in constitutive stimulation of the KRAS signaling pathway. KRAS signaling pathway activation has a high oncogenic potential and a very aggressive nature (102). For these reasons, the use of HCT116 and HT-29 cell lines enabled the comparison of a broad spectrum of features, which were characteristic of these types of cells. Furthermore, this allowed the present study to evaluate the therapeutic effects of an anticancer herbal component-based drug in combination with chemotherapy in CRC.

In the present study, UA and DOX significantly inhibited the proliferation, colony formation and migration of the human CRC HCT116 and HT-29 cell lines. It has been reported that DOX can arrest the cell cycle in G_1 phase in human CRC cells (103). Furthermore, cell cycle-associated regulators, such as CDKs and cyclins, dysregulation of which result in uncontrolled cellular proliferation and malignancy, are regulated by DOX (104). The present study demonstrated that UA enhanced DOX-mediated upregulation in the G_1 population of CRC cells. Apoptosis, a form of programmed cell death, is a promising target for anticancer therapy (105). Numerous treatments with natural products, such as herbal compounds, have been evaluated for their ability to induce cell apoptosis in CRC (106-109). Previous studies have assessed whether cell apoptosis is induced by UA in cancer, such as CRC and breast and esophageal cancer, via different mechanisms (27,110,111). The present study demonstrated that combined UA + DOX treatment promoted CRC cell late apoptosis and increased the sub-G_1 apoptotic fraction as assessed by FITC/PI staining and flow cytometry. UA + DOX promoted cleavage of PARP and activated caspase-9, which also suggested that combination treatment enhanced the effect on programmed cell death, compared with each drug alone.

The Akt signaling pathway serves a key role in tumorigenesis, and regulates cancer cell proliferation, migration and apoptosis (72). Overactivated PI3K/Akt signaling has been reported in numerous types of cancer, including CRC (112-114). Akt signaling pathway activation upregulates the expression of downstream genes c-Myc and cyclin D1 (115). Moreover, accumulating studies have reported that the Akt signaling pathway serves an important role in EMT and metastasis by inhibiting E-cadherin expression and upregulating the mesenchymal marker vimentin (116,117). Gsk3β is the downstream regulator of Akt signaling in malignant cells. Akt signaling inhibition has been reported to induce apoptosis via inhibition of Gsk3β (Ser9) by phosphorylation (118). Furthermore, there have been increasing reports that have suggested that

cyclin/CDKs, which act as the master regulator for cell cycle progression (119), are modulated by Gsk3β (120,121). In the present study, DOX markedly inhibited the protein expression levels of p-Akt and combination treatment further attenuated the activity of the Akt signaling pathway. These results demonstrated that the therapeutic effect primarily occurred via downregulation of the Akt signaling pathway and decreased the p-Gsk3β (S9) expression level following combined treatment in CRC cells. Consistent with these results, *in vivo* results demonstrated that UA and DOX treatment caused marked necrosis and morphological changes, and significantly decreased tumor volume compared with UA or DOX alone in the HCT116 xenograft tumor model. Moreover, the combination treatment at the dosage used in the present study did not significantly affect liver or kidney function, as evaluated by the detection of biochemical marker levels. Cardiotoxicity is the primary limitation of DOX-based chemotherapy (122). In a recent study, early protein markers of DOX toxicity were detected in mice treated with DOX at cumulative doses of ≥12 mg/kg (123). In the present study, low-dose DOX (2 mg/kg twice/week) treatment with a cumulative dose of <10 mg/kg was used and the heart was not assessed. However, serological analysis demonstrated that the dosage of UA and DOX did not significantly impair liver or kidney function. Therefore, these data suggested that UA and DOX treatment inhibited tumor progression without any toxicity to the liver or kidney at the endpoint of the animal experiment. Furthermore, the p-Akt/Akt protein expression levels were decreased in UA and DOX-treated xenograft animal tissue, which demonstrated that UA enhanced the efficacy of DOX by targeting the Akt signaling pathway, thus indicating that UA + DOX may serve as a potential therapeutic strategy for CRC.

The tumor-suppressive Hippo/Yap signaling pathway has attracted attention following reports that inhibits tumorigenesis (124-126). Activation of the Hippo/Yap signaling pathway primarily involves tumor suppressors (the Mst1/2 kinase cascade) and the following downstream regulators: following downstream regulators: Yap, transcriptional coactivator with PDZ postsynaptic density protein (TAZ), *Drosophila* disk large tumor suppressor and zonula occludens-1 protein-binding motif (127). It has been reported that tumor suppressor dysfunction and Yap activity overactivation can induce carcinogenesis, cancer proliferation and metastasis (128,129). Our previous study demonstrated that UA significantly upregulated the protein expression levels of tumor suppressors associated with the Hippo signaling pathway, such as Rassf1A, Mst1, Mst2 and Sav1 (130). In agreement with the aforementioned study, the present study demonstrated that DOX treatment stimulated the Hippo signaling pathway and UA markedly enhanced DOX-mediated activation of the Hippo signaling pathway both *in vivo* and *in vitro* and the activity of Yap was significantly inactivated by combination treatment in CRC cells. Numerous studies have reported the crosstalk between the Akt and Hippo/Yap signaling pathways in numerous types of cancer (131-136). For example, Akt has been reported to phosphorylate Mst1 and inhibit its activity, thereby preventing cell apoptosis (137). Upstream tumor suppressor phosphatase and tensin homolog inactivation has been reported to promote the PI3K/Akt signaling pathway in a Hippo pathway-dependent manner in human gastric cancer (136). Akt hyperactivation may inhibit the Hippo pathway and stabilize downstream transcriptional factor Yap/TAZ, thereby maintaining liver homeostasis (131). Previous studies regarding the Mst2 kinase reported that phosphorylation of Akt prevents Rassf1A binding and decreases Mst2 kinase activity (138,139). Rassf1A is a Hippo signaling pathway regulator that is highly silenced in human gastric (130), esophageal (140), lung (141), breast (142) and liver cancer (143). Akt signaling inhibition using a PI3K inhibitor can demethylate the promoter of Rassf1A and increase the protein expression levels of Rassf1A, resulting in Hippo signaling pathway activation (144,145). Therefore, inhibition of Akt is important for regulating the Hippo pathway on multiple levels. Notably, the present study indicated that the Akt signaling pathway was associated with the Hippo pathway and crosstalk occurred in CRC. There was no significant difference between UA + DOX combination treatment and SC79 + UA + DOX combination treatment in the expression levels of Akt/p-Akt and Hippo pathway proteins (Rassf1A, Mst1 and Sav1). The PI3K inhibitor LY294002 was used to assess the effects of the Akt signaling pathway and its association with the Hippo signaling pathway and UA and DOX-mediated anticancer effects. LY294002 further suppressed p-Akt expression, and induced Mst1/2, Sav1 and p-Yap expression, which led to decreased CTGF protein expression levels following UA and DOX combination treatment. In agreement with the *in vitro* data, the *in vivo* data demonstrated that the protein expression levels of p-Akt were significantly decreased, whereas Hippo pathway-associated protein expression levels (Rassf1A, Mst1, Mst2, Sav1, Mob1 and p-Mob1) were markedly increased in UA and DOX-treated xenograft mouse tumor samples.

In conclusion, these data indicated that Hippo signaling pathway stimulation may rely on Akt signaling pathway inhibition, with UA and DOX combination treatment effectively arresting tumor growth and metastasis, and triggering apoptosis in CRC cells. To delineate the molecular mechanisms and assess whether Akt directly or indirectly binds with tumor suppressors that serve a key role in the Hippo signaling pathway and affect the activation of downstream factors following UA and DOX treatment, a more in-depth study is required. Collectively, the present study demonstrated that a natural product-derived agent (UA) enhanced chemotherapy (DOX) outcomes by targeting PI3K/Akt signaling and activating the Hippo signaling pathway (Fig. 7), thus demonstrating the potential of UA in combination with DOX as a novel, more efficient strategy for CRC treatment.

Acknowledgements

Not applicable.

Funding

The present study was supported by The National University Development Project in 2020.

Availability of data and materials

The datasets used and/or analyzed during the current study are available from the corresponding author on reasonable request.

Authors' contributions

DH performed assays and wrote the manuscript. RYM performed analysis of the data. TVN and OHC performed H&E staining. BHP designed *in vivo* study and JSL performed the animal experiments. SMK conceived the experiments, and wrote and revised the manuscript. All authors have read and approved the final manuscript. DH and SMK confirm the authenticity of all the raw data.

Ethics approval and consent to participate

All animal care procedures and experiments were performed in accordance with the Animal Research: Reporting of *In Vivo* Experiments guidelines 2.0 and were approved by the Institutional Animal Care and Use Committee of Jeonbuk National University (approval no. CBNU2017-0001).

Patient consent for publication

Not applicable.

Competing interests

The authors declare that they have no competing interests.

References

1. Arnold M, Sierra MS, Laversanne M, Soerjomataram I, Jemal A and Bray F: Global patterns and trends in colorectal cancer incidence and mortality. Gut 66: 683-691, 2017.
2. Shin DW, Chang D, Jung JH, Han K, Kim SY, Choi KS, Lee WC, Park JH and Park JH: Disparities in the participation rate of colorectal cancer screening by fecal occult blood test among people with disabilities: A national database study in South Korea. Cancer Res Treat 52: 60-73, 2020.
3. Yang SY, Cho MS and Kim NK: Difference between right-sided and left-sided colorectal cancers: From embryology to molecular subtype. Expert Rev Anticancer Ther 18: 351-358, 2018.
4. McQuade RM, Stojanovska V, Bornstein JC and Nurgali K: Colorectal cancer chemotherapy: The evolution of treatment and new approaches. Curr Med Chem 24: 1537-1557, 2017.
5. Cargnin ST and Gnoatto SB: Ursolic acid from apple pomace and traditional plants: A valuable triterpenoid with functional properties. Food Chem 220: 477-489, 2017.
6. Xu C, Liao Y, Fang C, Tsunoda M, Zhang Y, Song Y and Deng S: Simultaneous analysis of ursolic acid and oleanolic acid in guava leaves using QuEChERS-based extraction followed by high-performance liquid chromatography. J Anal Methods Chem 2017: 2984562, 2017.
7. Zheng JL, Wang SS, Shen KP, Huang XW, Li M, Chen L, Peng X, An HM and Hu B: Ursolic acid potentiated oxaliplatin to induce apoptosis in colorectal cancer RKO cells. Pharmazie 75: 246-249, 2020.
8. Wang X, Wang T, Yi F, Duan C, Wang Q, He N, Zhu L, Li Q and Deng W: Ursolic acid inhibits tumor growth via epithelial-to-mesenchymal transition in colorectal cancer cells. Biol Pharm Bull 42: 685-691, 2019.
9. Cai Q, Lin J, Zhang L, Lin J, Wang L, Chen D and Peng J: Comparative proteomics-network analysis of proteins responsible for ursolic acid-induced cytotoxicity in colorectal cancer cells. Tumour Biol 39: 1010428317695015, 2017.
10. Wang C, Shu L, Zhang C, Li W, Wu R, Guo Y, Yang Y and Kong AN: Histone methyltransferase Setd7 regulates Nrf2 signaling pathway by phenethyl isothiocyanate and ursolic acid in human prostate cancer cells. Mol Nutr Food Res 62: e1700840, 2018.
11. Yang K, Chen Y, Zhou J, Ma L, Shan Y, Cheng X, Wang Y, Zhang Z, Ji X, Chen L, *et al*: Ursolic acid promotes apoptosis and mediates transcriptional suppression of CT45A2 gene expression in non-small-cell lung carcinoma harbouring EGFR T790M mutations. Br J Pharmacol 176: 4609-4624, 2019.
12. Mendes VIS, Bartholomeusz GA, Ayres M, Gandhi V and Salvador JAR: Synthesis and cytotoxic activity of novel A-ring cleaved ursolic acid derivatives in human non-small cell lung cancer cells. Eur J Med Chem 123: 317-331, 2016.
13. Chan EWC, Soon CY, Tan JBL, Wong SK and Hui YW: Ursolic acid: An overview on its cytotoxic activities against breast and colorectal cancer cells. J Integr Med 17: 155-160, 2019.
14. Kim K, Shin EA, Jung JH, Park JE, Kim DS, Shim BS and Kim SH: Ursolic acid induces apoptosis in colorectal cancer cells partially via upregulation of MicroRNA-4500 and inhibition of JAK2/STAT3 phosphorylation. Int J Mol Sci 20: 114, 2018.
15. Prasad S, Yadav VR, Sung B, Reuter S, Kannappan R, Deorukhkar A, Diagaradjane P, Wei C, Baladandayuthapani V, Krishnan S, *et al*: Ursolic acid inhibits growth and metastasis of human colorectal cancer in an orthotopic nude mouse model by targeting multiple cell signaling pathways: Chemosensitization with capecitabine. Clin Cancer Res 18: 4942-4953, 2012.
16. Liu P, Du R and Yu X: Ursolic acid exhibits potent anticancer effects in human metastatic melanoma cancer cells (SK-MEL-24) via apoptosis induction, inhibition of cell migration and invasion, cell cycle arrest, and inhibition of mitogen-activated protein kinase (MAPK)/ERK signaling pathway. Med Sci Monit 25: 1283-1290, 2019.
17. Liu T, Ma H, Shi W, Duan J, Wang Y, Zhang C, Li C, Lin J, Li S, Lv J and Lin L: Inhibition of STAT3 signaling pathway by ursolic acid suppresses growth of hepatocellular carcinoma. Int J Oncol 51: 555-562, 2017.
18. Zhang L, Cai QY, Liu J, Peng J, Chen YQ, Sferra TJ and Lin JM: Ursolic acid suppresses the invasive potential of colorectal cancer cells by regulating the TGF-β1/ZEB1/miR-200c signaling pathway. Oncol Lett 18: 3274-3282, 2019.
19. Cheng J, Liu Y, Liu Y, Liu D, Liu Y, Guo Y, Wu Z, Li H and Wang H: Ursolic acid alleviates lipid accumulation by activating the AMPK signaling pathway in vivo and in vitro. J Food Sci 85: 3998-4008, 2020.
20. Kim GH, Kan SY, Kang H, Lee S, Ko HM, Kim JH and Lim JH: Ursolic acid suppresses cholesterol biosynthesis and exerts anti-cancer effects in hepatocellular carcinoma cells. Int J Mol Sci 20: 4767, 2019.
21. Lin CW, Chin HK, Lee SL, Chiu CF, Chung JG, Lin ZY, Wu CY, Liu YC, Hsiao YT, Feng CH, *et al*: Ursolic acid induces apoptosis and autophagy in oral cancer cells. Environ Toxicol 34: 983-991, 2019.
22. Lin JH, Chen SY, Lu CC, Lin JA and Yen GC: Ursolic acid promotes apoptosis, autophagy, and chemosensitivity in gemcitabine-resistant human pancreatic cancer cells. Phytother Res 34: 2053-2066, 2020.
23. Lin W and Ye H: Anticancer activity of ursolic acid on human ovarian cancer cells via ROS and MMP mediated apoptosis, cell cycle arrest and downregulation of PI3K/AKT pathway. J BUON 25: 750-756, 2020.
24. Li W, Zhang H, Nie M, Tian Y, Chen X, Chen C, Chen H and Liu R: Ursolic acid derivative FZU-03,010 inhibits STAT3 and induces cell cycle arrest and apoptosis in renal and breast cancer cells. Acta Biochim Biophys Sin (Shanghai) 49: 367-373, 2017.
25. Ruan JS, Zhou H, Yang L, Wang L, Jiang ZS, Sun H and Wang SM: Ursolic acid attenuates TGF-β1-induced epithelial-mesenchymal transition in NSCLC by targeting integrin αVβ5/MMPs signaling. Oncol Res 27: 593-600, 2019.
26. Sohn EJ, Won G, Lee J, Yoon SW, Lee I, Kim HJ and Kim SH: Blockage of epithelial to mesenchymal transition and upregulation of let 7b are critically involved in ursolic acid induced apoptosis in malignant mesothelioma cell. Int J Biol Sci 12: 1279-1288, 2016.
27. Lee NR, Meng RY, Rah SY, Jin H, Ray N, Kim SH, Park BH and Kim SM: Reactive oxygen species-mediated autophagy by ursolic acid inhibits growth and metastasis of esophageal cancer cells. Int J Mol Sci 21: 9409, 2020.
28. Park HJ, Jo DS, Choi DS, Bae JE, Park NY, Kim JB, Chang JH, Shin JJ and Cho DH: Ursolic acid inhibits pigmentation by increasing melanosomal autophagy in B16F1 cells. Biochem Biophys Res Commun 531: 209-214, 2020.
29. Arcamone F, Cassinelli G, Fantini G, Grein A, Orezzi P, Pol C and Spalla C: Adriamycin, 14-hydroxydaunomycin, a new antitumor antibiotic from S. peucetius var. caesius. Reprinted from biotechnology and bioengineering, Vol. XI, Issue 6, Pages 1101-1110 (1969). Biotechnol Bioeng 67: 704-713, 2000.
30. Cortés-Funes H and Coronado C: Role of anthracyclines in the era of targeted therapy. Cardiovasc Toxicol 7: 56-60, 2007.

31. Weiss RB: The anthracyclines: Will we ever find a better doxorubicin? Semin Oncol 19: 670-686, 1992.
32. Sarmento-Ribeiro AB, Scorilas A, Goncalves AC, Efferth T and Trougakos IP: The emergence of drug resistance to targeted cancer therapies: Clinical evidence. Drug Resist Updat 47: 100646, 2019.
33. Rui M, Xin Y, Li R, Ge Y, Feng C and Xu X: Targeted biomimetic nanoparticles for synergistic combination chemotherapy of paclitaxel and doxorubicin. Mol Pharm 14: 107-123, 2017.
34. Fan YP, Liao JZ, Lu YQ, Tian DA, Ye F, Zhao PX, Xiang GY, Tang WX and He XX: MiR-375 and doxorubicin co-delivered by liposomes for combination therapy of hepatocellular carcinoma. Mol Ther Nucleic Acids 7: 181-189, 2017.
35. Minotti G, Menna P, Salvatorelli E, Cairo G and Gianni L: Anthracyclines: Molecular advances and pharmacologic developments in antitumor activity and cardiotoxicity. Pharmacol Rev 56: 185-229, 2004.
36. Guo NF, Cao YJ, Chen X, Zhang Y, Fan YP, Liu J and Chen XL: Lixisenatide protects doxorubicin-induced renal fibrosis by activating wNF-κB/TNF-α and TGF-β/Smad pathways. Eur Rev Med Pharmacol Sci 23: 4017-4026, 2019.
37. Saleh D, Abdelbaset M, Hassan A, Sharaf O, Mahmoud S and Hegazy R: Omega-3 fatty acids ameliorate doxorubicin-induced cardiorenal toxicity: In-vivo regulation of oxidative stress, apoptosis and renal Nox4, and in-vitro preservation of the cytotoxic efficacy. PLoS One 15: e0242175, 2020.
38. Prasanna PL, Renu K and Valsala Gopalakrishnan A: New molecular and biochemical insights of doxorubicin-induced hepatotoxicity. Life Sci 250: 117599, 2020.
39. Zhou X, Xu P, Dang R, Guo Y, Li G, Qiao Y, Xie R, Liu Y and Jiang P: The involvement of autophagic flux in the development and recovery of doxorubicin-induced neurotoxicity. Free Radic Biol Med 129: 440-445, 2018.
40. Yu FX, Zhao B and Guan KL: Hippo pathway in organ size control, tissue homeostasis, and cancer. Cell 163: 811-828, 2015.
41. Kim CL, Choi SH and Mo JS: Role of the Hippo pathway in fibrosis and cancer. Cells 8: 468, 2019.
42. Dong J, Feldmann G, Huang J, Wu S, Zhang N, Comerford SA, Gayyed MF, Anders RA, Maitra A and Pan D: Elucidation of a universal size-control mechanism in *Drosophila* and mammals. Cell 130: 1120-1233, 2007.
43. Avruch J, Zhou D and Bardeesy N: YAP oncogene overexpression supercharges colon cancer proliferation. Cell Cycle 11: 1090-1096, 2012.
44. Liu XF, Han Q, Rong XZ, Yang M, Han YC, Yu JH and Lin XY: ANKHD1 promotes proliferation and invasion of non-small-cell lung cancer cells via regulating YAP oncoprotein expression and inactivating the Hippo pathway. Int J Oncol 56: 1175-1185, 2020.
45. Niu K, Liu Y, Zhou Z, Wu X, Wang H and Yan J: Antitumor effects of paeoniflorin on Hippo signaling pathway in gastric cancer cells. J Oncol 2021: 4724938, 2021.
46. Hou L, Chen L and Fang L: Scutellarin inhibits proliferation, invasion, and tumorigenicity in human breast cancer cells by regulating HIPPO-YAP signaling pathway. Med Sci Monit 23: 5130-5138, 2017.
47. Driskill JH and Pan D: The Hippo pathway in liver homeostasis and pathophysiology. Annu Rev Pathol 16: 299-322, 2021.
48. Masliantsev K, Karayan-Tapon L and Guichet PO: Hippo signaling pathway in gliomas. Cells 10: 184, 2021.
49. Ansari D, Ohlsson H, Althini C, Bauden M, Zhou Q, Hu D and Andersson R: The Hippo signaling pathway in pancreatic cancer. Anticancer Res 39: 3317-3321, 2019.
50. Llado V, Nakanishi Y, Duran A, Reina-Campos M, Shelton PM, Linares JF, Yajima T, Campos A, Aza-Blanc P, Leitges M, *et al*: Repression of intestinal stem cell function and tumorigenesis through direct phosphorylation of β-catenin and Yap by PKCζ. Cell Rep 10: 740-754, 2015.
51. Chen L, Qin F, Deng X, Avruch J and Zhou D: Hippo pathway in intestinal homeostasis and tumorigenesis. Protein Cell 3: 305-310, 2012.
52. Gu Y, Zhang L and Yu FX: Functions and regulations of the Hippo signaling pathway in intestinal homeostasis, regeneration and tumorigenesis. Yi Chuan 39: 588-596, 2017.
53. Zhou D, Zhang Y, Wu H, Barry E, Yin Y, Lawrence E, Dawson D, Willis JE, Markowitz SD, Camargo FD and Avruch J: Mst1 and Mst2 protein kinases restrain intestinal stem cell proliferation and colonic tumorigenesis by inhibition of Yes-associated protein (Yap) overabundance. Proc Natl Acad Sci USA 108: E1312-E1320, 2011.
54. Xiao Y, Liu Q, Peng N, Li Y, Qiu D, Yang T, Kang R, Usmani A, Amadasu E, Borlongan CV and Yu G: Lovastatin inhibits RhoA to suppress canonical Wnt/β-catenin signaling and alternative Wnt-YAP/TAZ signaling in colon cancer. Cell Transplant 31: 9636897221075749, 2022.
55. Touil Y, Igoudjil W, Corvaisier M, Dessein AF, Vandomme J, Monté D, Stechly L, Skrypek N, Langlois C, Grard G, *et al*: Colon cancer cells escape 5FU chemotherapy-induced cell death by entering stemness and quiescence associated with the c-Yes/YAP axis. Clin Cancer Res 20: 837-846, 2014.
56. Shamekhi S, Abdolalizadeh J, Ostadrahimi A, Mohammadi SA, Barzegari A, Lotfi H, Bonabi E and Zarghami N: Apoptotic effect of saccharomyces cerevisiae on human colon cancer SW480 cells by regulation of Akt/NF-κB signaling pathway. Probiotics Antimicrob Proteins 12: 311-319, 2020.
57. Goel S, Huang J and Klampfer L: K-Ras, intestinal homeostasis and colon cancer. Curr Clin Pharmacol 10: 73-81, 2015.
58. Tumaneng K, Schlegelmilch K, Russell RC, Yimlamai D, Basnet H, Mahadevan N, Fitamant J, Bardeesy N, Camargo FD and Guan KL: YAP mediates crosstalk between the Hippo and PI(3)K-TOR pathways by suppressing PTEN via miR-29. Nat Cell Biol 14: 1322-1329, 2012.
59. Yu FX, Zhao B, Panupinthu N, Jewell JL, Lian I, Wang LH, Zhao J, Yuan H, Tumaneng K, Li H, *et al*: Regulation of the Hippo-YAP pathway by G-protein-coupled receptor signaling. Cell 150: 780-791, 2012.
60. Kawai K, Viars C, Arden K, Tarin D, Urquidi V and Goodison S: Comprehensive karyotyping of the HT-29 colon adenocarcinoma cell line. Genes Chromosomes Cancer 34: 1-8, 2002.
61. Grada A, Otero-Vinas M, Prieto-Castrillo F, Obagi Z and Falanga V: Research techniques made simple: Analysis of collective cell migration using the wound healing assay. J Invest Dermatol 137: e11-e16, 2017.
62. Vang Mouritzen M and Jenssen H: Optimized scratch assay for in vitro testing of cell migration with an automated optical camera. J Vis Exp: 57691, 2018.
63. Martinotti S and Ranzato E: Scratch wound healing assay. Methods Mol Biol 2109: 225-229, 2020.
64. Meng RY, Jin H, Nguyen TV, Chai OH, Park BH and Kim SM: Ursolic acid accelerates paclitaxel-induced cell death in esophageal cancer cells by suppressing Akt/FOXM1 signaling cascade. Int J Mol Sci 22: 11486, 2021.
65. Stephenson W: Deficiencies in the national institute of health's guidelines for the care and protection of laboratory animals. J Med Philos 18: 375-88, 1993.
66. Kilkenny C, Browne WJ, Cuthill IC, Emerson M and Altman DG: Improving bioscience research reporting: The ARRIVE guidelines for reporting animal research. Osteoarthritis Cartilage 20: 256-260, 2012.
67. Spangenberg EM and Keeling LJ: Assessing the welfare of laboratory mice in their home environment using animal-based measures-a benchmarking tool. Lab Anim 50: 30-38, 2016.
68. Clayden EC: Practical section cutting and staining. 5th edition. Edinburgh: (15 Teviot Place, Edinburgh 1), Churchill Livingstone, 7: pp270, 1971.
69. Kim DH, Kang DY, Sp N, Jo ES, Rugamba A, Jang KJ and Yang YM: Methylsulfonylmethane induces cell cycle arrest and apoptosis, and suppresses the stemness potential of HT-29 cells. Anticancer Res 40: 5191-5200, 2020.
70. Ombrato L and Malanchi I: The EMT universe: Space between cancer cell dissemination and metastasis initiation. Crit Rev Oncog 19: 349-361, 2014.
71. Wang C, Li Z, Lu Y, Du R, Katiyar S, Yang J, Fu M, Leader JE, Quong A, Novikoff PM and Pestell RG: Cyclin D1 repression of nuclear respiratory factor 1 integrates nuclear DNA synthesis and mitochondrial function. Proc Natl Acad Sci USA 103: 11567-11572, 2006.
72. Bishnupuri KS, Alvarado DM, Khouri AN, Shabsovich M, Chen B, Dieckgraefe BK and Ciorba MA: IDO1 and kynurenine pathway metabolites activate PI3K-Akt signaling in the neoplastic colon epithelium to promote cancer cell proliferation and inhibit apoptosis. Cancer Res 79: 1138-1150, 2019.
73. Ji J, Wang Z, Sun W, Li Z, Cai H, Zhao E and Cui H: Effects of cynaroside on cell proliferation, apoptosis, migration and invasion though the MET/AKT/mTOR axis in gastric cancer. Int J Mol Sci 22: 12125, 2021.
74. Zhang P, Yuan X, Yu T, Huang H, Yang C, Zhang L, Yang S, Luo X and Luo J: Lycorine inhibits cell proliferation, migration and invasion, and primarily exerts *in vitro* cytostatic effects in human colorectal cancer via activating the ROS/p38 and AKT signaling pathways. Oncol Rep 45: 19, 2021.

75. Yang L, Liu Y, Wang M, Qian Y, Dong X, Gu H, Wang H, Guo S and Hisamitsu T: Quercetin-induced apoptosis of HT-29 colon cancer cells via inhibition of the Akt-CSN6-Myc signaling axis. Mol Med Rep 14: 4559-4566, 2016.
76. Guo C, Zhang X and Pfeifer GP: The tumor suppressor RASSF1A prevents dephosphorylation of the mammalian STE20-like kinases MST1 and MST2. J Biol Chem 286: 6253-6261, 2011.
77. Kim M, Kim M, Lee MS, Kim CH and Lim DS: The MST1/2-SAV1 complex of the Hippo pathway promotes ciliogenesis. Nat Commun 5: 5370, 2014.
78. Shome D, von Woedtke T, Riedel K and Masur K: The HIPPO transducer YAP and its targets CTGF and Cyr61 drive a paracrine signalling in cold atmospheric plasma-mediated wound healing. Oxid Med Cell Longev 2020: 4910280, 2020.
79. Wang Y, Kuramitsu Y, Baron B, Kitagawa T, Tokuda K, Akada J, Maehara SI, Maehara Y and Nakamura K: PI3K inhibitor LY294002, as opposed to wortmannin, enhances AKT phosphorylation in gemcitabine-resistant pancreatic cancer cells. Int J Oncol 50: 606-612, 2017.
80. Lin J, Chen Y, Wei L, Hong Z, Sferra TJ and Peng J: Ursolic acid inhibits colorectal cancer angiogenesis through suppression of multiple signaling pathways. Int J Oncol 43: 1666-1674, 2013.
81. Zhang Y, Huang L, Shi H, Chen H, Tao J, Shen R and Wang T: Ursolic acid enhances the therapeutic effects of oxaliplatin in colorectal cancer by inhibition of drug resistance. Cancer Sci 109: 94-102, 2018.
82. Zeng Q, Che Y, Zhang Y, Chen M, Guo Q and Zhang W: Thymol isolated from thymus vulgaris L. inhibits colorectal cancer cell growth and metastasis by suppressing the Wnt/β-catenin pathway. Drug Des Devel Ther 14: 2535-2547, 2020.
83. Yao M, Ma X, Zhang X, Shi L, Liu T, Liang X, Zhao H, Li X, Li L, Gao H, *et al*: Lectin-mediated pH-sensitive doxorubicin prodrug for pre-targeted chemotherapy of colorectal cancer with enhanced efficacy and reduced side effects. Theranostics 9: 747-760, 2019.
84. O'Bryan RM, Baker LH, Gottlieb JE, Rivkin SE, Balcerzak SP, Grumet GN, Salmon SE, Moon TE and Hoogstraten B: Dose response evaluation of adriamycin in human neoplasia. Cancer 39: 1940-1948, 1977.
85. Gabizon A, Shmeeda H and Barenholz Y: Pharmacokinetics of pegylated liposomal doxorubicin: Review of animal and human studies. Clin Pharmacokinet 42: 419-436, 2003.
86. Marina NM, Cochrane D, Harney E, Zomorodi K, Blaney S, Winick N, Bernstein M and Link MP: Dose escalation and pharmacokinetics of pegylated liposomal doxorubicin (Doxil) in children with solid tumors: A pediatric oncology group study. Clin Cancer Res 8: 413-418, 2002.
87. Nair AB and Jacob S: A simple practice guide for dose conversion between animals and human. J Basic Clin Pharm 7: 27-31, 2016.
88. Siegel RL, Miller KD and Jemal A: Cancer statistics, 2019. CA Cancer J Clin 69: 7-34, 2019.
89. Xie YH, Chen YX and Fang JY: Comprehensive review of targeted therapy for colorectal cancer. Signal Transduct Target Ther 5: 22, 2020.
90. Li J, Ma X, Chakravarti D, Shalapour S and DePinho RA: Genetic and biological hallmarks of colorectal cancer. Genes Dev 35: 787-820, 2021.
91. Tiwari A, Saraf S, Verma A, Panda PK and Jain SK: Novel targeting approaches and signaling pathways of colorectal cancer: An insight. World J Gastroenterol 24: 4428-4435, 2018.
92. Krishnamurthy N and Kurzrock R: Targeting the Wnt/beta-catenin pathway in cancer: Update on effectors and inhibitors. Cancer Treat Rev 62: 50-60, 2018.
93. Chen Z, Oh D, Dubey AK, Yao M, Yang B, Groves JT and Sheetz M: EGFR family and Src family kinase interactions: Mechanics matters? Curr Opin Cell Biol 51: 97-102, 2018.
94. Lopez A, Harada K, Vasilakopoulou M, Shanbhag N and Ajani JA: Targeting angiogenesis in colorectal carcinoma. Drugs 79: 63-74, 2019.
95. Ahmad R, Singh JK, Wunnava A, Al-Obeed O, Abdulla M and Srivastava SK: Emerging trends in colorectal cancer: Dysregulated signaling pathways (Review). Int J Mol Med 47: 14, 2021.
96. Kassi E, Sourlingas TG, Spiliotaki M, Papoutsi Z, Pratsinis H, Aligiannis N and Moutsatsou P: Ursolic acid triggers apoptosis and Bcl-2 downregulation in MCF-7 breast cancer cells. Cancer Invest 27: 723-733, 2009.
97. Yim EK, Lee KH, Namkoong SE, Um SJ and Park JS: Proteomic analysis of ursolic acid-induced apoptosis in cervical carcinoma cells. Cancer Lett 235: 209-220, 2006.
98. Argenziano M, Gigliotti CL, Clemente N, Boggio E, Ferrara B, Trotta F, Pizzimenti S, Barrera G, Boldorini R, Bessone F, *et al*: Improvement in the anti-tumor efficacy of doxorubicin nanosponges in in vitro and in mice bearing breast tumor models. Cancers (Basel) 12: 162, 2020.
99. Brattain MG, Brattain DE, Fine WD, Khaled FM, Marks ME, Kimball PM, Arcolano LA and Danbury BH: Initiation and characterization of cultures of human colonic carcinoma with different biological characteristics utilizing feeder layers of confluent fibroblasts. Oncodev Biol Med 2: 355-366, 1981.
100. Brattain MG, Fine WD, Khaled FM, Thompson J and Brattain DE: Heterogeneity of malignant cells from a human colonic carcinoma. Cancer Res 41: 1751-1756, 1981.
101. Ahmed D, Eide PW, Eilertsen IA, Danielsen SA, Eknaes M, Hektoen M, Lind GE and Lothe RA: Epigenetic and genetic features of 24 colon cancer cell lines. Oncogenesis 2: e71, 2013.
102. Bazan V, Migliavacca M, Zanna I, Tubiolo C, Grassi N, Latteri MA, La Farina M, Albanese I, Dardanoni G, Salerno S, *et al*: Specific codon 13 K-ras mutations are predictive of clinical outcome in colorectal cancer patients, whereas codon 12 K-ras mutations are associated with mucinous histotype. Ann Oncol 13: 1438-1446, 2002.
103. Lupertz R, Watjen W, Kahl R and Chovolou Y: Dose- and time-dependent effects of doxorubicin on cytotoxicity, cell cycle and apoptotic cell death in human colon cancer cells. Toxicology 271: 115-121, 2010.
104. Nie W, Zan X, Yu T, Ran M, Hong Z, He Y, Yang T, Ju Y and Gao X: Synergetic therapy of glioma mediated by a dual delivery system loading α-mangostin and doxorubicin through cell cycle arrest and apoptotic pathways. Cell Death Dis 11: 928, 2020.
105. Tilija Pun N, Jang WJ and Jeong CH: Role of autophagy in regulation of cancer cell death/apoptosis during anti-cancer therapy: Focus on autophagy flux blockade. Arch Pharm Res 43: 475-488, 2020.
106. Lin YJ, Liang WM, Chen CJ, Tsang H, Chiou JS, Liu X, Cheng CF, Lin TH, Liao CC, Huang SM, *et al*: Network analysis and mechanisms of action of Chinese herb-related natural compounds in lung cancer cells. Phytomedicine 58: 152893, 2019.
107. Doğan Şiğva ZÖ, Balci Okcanoğlu T, Biray Avci Ç, Yilmaz Süslüer S, Kayabaşi Ç, Turna B, Dodurga Y, Nazli O and Gündüz C: Investigation of the synergistic effects of paclitaxel and herbal substances and endemic plant extracts on cell cycle and apoptosis signal pathways in prostate cancer cell lines. Gene 687: 261-271, 2019.
108. Aiello P, Sharghi M, Mansourkhani SM, Ardekan AP, Jouybari L, Daraei N, Peiro K, Mohamadian S, Rezaei M, Heidari M, *et al*: Medicinal plants in the prevention and treatment of colon cancer. Oxid Med Cell Longev 2019: 2075614, 2019.
109. Phan T, Nguyen VH, A'Lincourt Salazar M, Wong P, Diamond DJ, Yim JH and Melstrom LG: Inhibition of autophagy amplifies baicalein-induced apoptosis in human colorectal cancer. Mol Ther Oncolytics 19: 1-7, 2020.
110. Mandal S, Gamit N, Varier L, Dharmarajan A and Warrier S: Inhibition of breast cancer stem-like cells by a triterpenoid, ursolic acid, via activation of Wnt antagonist, sFRP4 and suppression of miRNA-499a-5p. Life Sci 265: 118854, 2021.
111. Zheng JL, Wang SS, Shen KP, Chen L, Peng X, Chen JF, An HM and Hu B: Ursolic acid induces apoptosis and anoikis in colorectal carcinoma RKO cells. BMC Complement Med Ther 21: 52, 2021.
112. Yang S, Zhang X, Qu H, Qu B, Yin X and Zhao H: Cabozantinib induces PUMA-dependent apoptosis in colon cancer cells via AKT/GSK-3β/NF-κB signaling pathway. Cancer Gene Ther 27: 368-377, 2020.
113. Qin J, Fu M, Wang J, Huang F, Liu H, Huangfu M, Yu D, Liu H, Li X, Guan X and Chen X: PTEN/AKT/mTOR signaling mediates anticancer effects of epigallocatechin-3-gallate in ovarian cancer. Oncol Rep 43: 1885-1896, 2020.
114. Zhu ML, Zhang PM, Jiang M, Yu SW and Wang L: Myricetin induces apoptosis and autophagy by inhibiting PI3K/Akt/mTOR signalling in human colon cancer cells. BMC Complement Med Ther 20: 209, 2020.
115. Li W, Li C, Ma L and Jin F: Resveratrol inhibits viability and induces apoptosis in the small-cell lung cancer H446 cell line via the PI3K/Akt/c-Myc pathway. Oncol Rep 44: 1821-1830, 2020.

116. Tian J, Zhang H, Mu L, Wang M, Li X, Zhang X, Xie E, Ma M, Wu D and Du Y: The miR-218/GAB2 axis regulates proliferation, invasion and EMT via the PI3K/AKT/GSK-3β pathway in prostate cancer. Exp Cell Res 394: 112128, 2020.
117. Qi X, Sun L, Wan J, Xu R, He S and Zhu X: Tensin4 promotes invasion and migration of gastric cancer cells via regulating AKT/GSK-3β/snail signaling pathway. Pathol Res Pract 216: 153001, 2020.
118. Chang YX, Lin YF, Chen CL, Huang MS, Hsiao M and Liang PH: Chaperonin-containing TCP-1 promotes cancer chemoresistance and metastasis through the AKT-GSK3β-β-catenin and XIAP-survivin pathways. Cancers (Basel) 12: 3865, 2020.
119. Ding L, Cao J, Lin W, Chen H, Xiong X, Ao H, Yu M, Lin J and Cui Q: The roles of cyclin-dependent kinases in cell-cycle progression and therapeutic strategies in human breast cancer. Int J Mol Sci 21: 1960, 2020.
120. Xu S, Zhang H, Liu T, Yang W, Lv W, He D, Guo P and Li L: 6-Gingerol induces cell-cycle G1-phase arrest through AKT-GSK 3β-cyclin D1 pathway in renal-cell carcinoma. Cancer Chemother Pharmacol 85: 379-390, 2020.
121. Zhou C, Du J, Zhao L, Liu W, Zhao T, Liang H, Fang P, Zhang K and Zeng H: GLI1 reduces drug sensitivity by regulating cell cycle through PI3K/AKT/GSK3/CDK pathway in acute myeloid leukemia. Cell Death Dis 12: 231, 2021.
122. Zhang S, Liu X, Bawa-Khalfe T, Lu LS, Lyu YL, Liu LF and Yeh ET: Identification of the molecular basis of doxorubicin-induced cardiotoxicity. Nat Med 18: 1639-1642, 2012.
123. Desai VG, Lee T, Moland CL, Vijay V, Han T, Lewis SM, Herman EH and Fuscoe JC: Candidate early predictive plasma protein markers of doxorubicin-induced chronic cardiotoxicity in B6C3F$_1$ mice. Toxicol Appl Pharmacol 363: 164-173, 2019.
124. Kuenzi BM and Ideker T: Author correction: A census of pathway maps in cancer systems biology. Nat Rev Cancer 21: 212, 2021.
125. Kuenzi BM and Ideker T: A census of pathway maps in cancer systems biology. Nat Rev Cancer 20: 233-246, 2020.
126. Chang YC, Wu JW, Wang CW and Jang AC: Hippo signaling-mediated mechanotransduction in cell movement and cancer metastasis. Front Mol Biosci 6: 157, 2020.
127. Kennedy MB: Origin of PDZ (DHR, GLGF) domains. Trends Biochem Sci 20: 350, 1995.
128. Zheng Y and Pan D: The Hippo signaling pathway in development and disease. Dev Cell 50: 264-282, 2019.
129. Furth N and Aylon Y: The LATS1 and LATS2 tumor suppressors: Beyond the Hippo pathway. Cell Death Differ 24: 1488-1501, 2017.
130. Kim SH, Jin H, Meng RY, Kim DY, Liu YC, Chai OH, Park BH and Kim SM: Activating Hippo pathway via Rassf1 by ursolic acid suppresses the tumorigenesis of gastric cancer. Int J Mol Sci 20: 4709, 2019.
131. Jeong SH, Kim HB, Kim MC, Lee JM, Lee JH, Kim JH, Kim JW, Park WY, Kim SY, Kim JB, *et al*: Hippo-mediated suppression of IRS2/AKT signaling prevents hepatic steatosis and liver cancer. J Clin Invest 128: 1010-1025, 2018.
132. Zhang S, Chen Q, Liu Q, Li Y, Sun X, Hong L, Ji S, Liu C, Geng J, Zhang W, *et al*: Hippo signaling suppresses cell ploidy and tumorigenesis through Skp2. Cancer Cell 31: 669-684.e7, 2017.
133. Ahmed AA, Abedalthagafi M, Anwar AE and Bui MM: Akt and Hippo pathways in Ewing's sarcoma tumors and their prognostic significance. J Cancer 6: 1005-1010, 2015.
134. Berthold R, Isfort I, Erkut C, Heinst L, Grunewald I, Wardelmann E, Kindler T, Åman P, Grünewald TGP, Cidre-Aranaz F, *et al*: Fusion protein-driven IGF-IR/PI3K/AKT signals deregulate Hippo pathway promoting oncogenic cooperation of YAP1 and FUS-DDIT3 in myxoid liposarcoma. Oncogenesis 11: 20, 2022.
135. Ma W, Han C, Zhang J, Song K, Chen W, Kwon H and Wu T: The histone methyltransferase G9a promotes cholangiocarcinogenesis through regulation of the Hippo pathway kinase LATS2 and YAP signaling pathway. Hepatology 72: 1283-1297, 2020.
136. Xu W, Yang Z, Xie C, Zhu Y, Shu X, Zhang Z, Li N, Chai N, Zhang S, Wu K, *et al*: PTEN lipid phosphatase inactivation links the hippo and PI3K/Akt pathways to induce gastric tumorigenesis. J Exp Clin Cancer Res 37: 198, 2018.
137. Jang SW, Yang SJ, Srinivasan S and Ye K: Akt phosphorylates MstI and prevents its proteolytic activation, blocking FOXO3 phosphorylation and nuclear translocation. J Biol Chem 282: 30836-30844, 2007.
138. Romano D, Matallanas D, Weitsman G, Preisinger C, Ng T and Kolch W: Proapoptotic kinase MST2 coordinates signaling crosstalk between RASSF1A, Raf-1, and Akt. Cancer Res 70: 1195-1203, 2010.
139. Kim D, Shu S, Coppola MD, Kaneko S, Yuan ZQ and Cheng JQ: Regulation of proapoptotic mammalian ste20-like kinase MST2 by the IGF1-Akt pathway. PLoS One 5: e9616, 2010.
140. Kim SM, Ye S, Rah SY, Park BH, Wang H, Kim JR, Kim SH, Jang KY and Lee KB: RhBMP-2 activates Hippo signaling through RASSF1 in esophageal cancer cells. Sci Rep 6: 26821, 2016.
141. Pankova D, Jiang Y, Chatzifrangkeskou M, Vendrell I, Buzzelli J, Ryan A, Brown C and O'Neill E: RASSF1A controls tissue stiffness and cancer stem-like cells in lung adenocarcinoma. EMBO J 38: e100532, 2019.
142. Gupta V, Agarwal P and Deshpande P: Impact of RASSF1A gene methylation on clinico-pathological features of tumor and non-tumor tissue of breast cancer. Ann Diagn Pathol 52: 151722, 2021.
143. Lee NH, Kim SJ and Hyun J: MicroRNAs regulating Hippo-YAP signaling in liver cancer. Biomedicines 9: 347, 2021.
144. Agarwal S, Amin KS, Jagadeesh S, Baishay G, Rao PG, Barua NC, Bhattacharya S and Banerjee PP: Mahanine restores RASSF1A expression by down-regulating DNMT1 and DNMT3B in prostate cancer cells. Mol Cancer 12: 99, 2013.
145. Blanchard TG, Lapidus R, Banerjee V, Bafford AC, Czinn SJ, Ahmed H and Banerjee A: Upregulation of RASSF1A in colon cancer by suppression of angiogenesis signaling and Akt activation. Cell Physiol Biochem 48: 1259-1273, 2018.